# RESOLVING CYCLE SKIP INTRODUCED BY THE MULTI-LAYER STATIC MODEL USING A HYBRID APPROACH

BY

Emad Ekladios Toma Tawadros

A Thesis Presented to the

DEANSHIP OF GRADUATE STUDIES

**KING FAHD UNIVERSITY OF PETROLEUM & MINERALS**

DHAHRAN, SAUDI ARABIA

In Partial Fulfillment of the

Requirements for the Degree of

**MASTER OF SCIENCE**

**In**

**GEOPHYSICS**

**May, 2011**

To my beloved

parents, wife, kids and siblings.

## ACKNOWLEDGMENT

Acknowledgment is due to the King Fahd University of Petroleum & Minerals for supporting this research.

I wish to express my appreciation to *Dr. Abdullatif Al-Shuhail* who served as my major advisor for his continuous, valuable guidance and patience throughout the course of this research work. I also wish to thank my thesis committee members *Dr. Sanlinn Ismail Kaka* and *Dr. Giulio Vignoli* for their valuable support and feedback.

Special thanks for Saudi Aramco represented by Geophysical Data Processing Division for acquiring the seismic data. Thanks to Mr. Ralph Bridle and Mr. Robert Wilson Rowe for their suggestions and support.

# TABLE OF CONTENTS

**Page**

**LIST OF FIGURES**..... **vi**

**ABSTRACT (ARABIC)**..... **IX**

**ABSTRACT (ENGLISH)**..... **X**

**CHAPTER1. INTRODUCTION**..... **01**

1.1 INTRODUCTION..... 01

1.2 PROBLEM STATEMENT..... 03

1.3 THE CAUSES..... 12

1.3.1 BURIED ANOMALIES..... 15

1.3.2 VELOCITY INVERSIONS..... 19

1.3.3 COMPLEX REFRACTORS..... 27

**CHAPTER2. OBJECTIVE**..... **29**

2.1 INTRODUCTION..... 29

2.2 CONCEPT..... 30

2.3 DATA PROCESSING..... 34

**CHAPTER3. METHODOLOGY**..... **36**

3.1 INTRODUCTION..... 36

3.2 CONVENTIONAL METHODOLOGY..... 36

3.3 PROPOSED METHODOLOGY..... 44

**CHAPTER4. RESULTS**..... **48**

4.1 INTRODUCTION..... 48

4.2 PRE-STACK DATA..... 48

4.3 POST-STACK DATA..... 48

**CHAPTER5. CONCLUSION & RECOMMENDATION**..... **56**

5.1 CONCLUSION..... 56

5.2 RECOMMENDATION..... 57

**BIBLIOGRAPHY**..... **59**

**VITA**..... **61**

# LIST OF FIGURES

*Figure 1.1: Partitioning of total statics, high frequency and low Frequency components……. 02*

*Figure 1.2: Areal dimensions of 3D area under study ……. 05*

*Figure 1.3: Time slice at 1400 ms, conventional static solution (multi-layer model and internal pilot residual statics applied) ……. 06*

*Figure 1.4: Cross-line (A) stack with the high frequency statics of the single layer model…... 07*

*Figure 1.5: Cross-line (A) stack with the high frequency statics of the multi-layer model…... 08*

*Figure 1.6: Inline (B) stack with the high frequency statics of the single layer model…….. 09*

*Figure 1.7: Inline (A) stack with the high frequency statics of the multi-layer model…….. 10*

*Figure 1.8: An example shot record, conventional static solution (multi-layer applied)…… 11*

*Figure 1.9: Earth model, two ray paths travelling just below refractors at velocities of V1 and V2…….. 13*

*Figure 1.10: An uphole records near vertical ray paths……. 14*

*Figure 1.11: Effect of buried anomalies, on the refracted ray paths travelling just below refractors at velocities of V1 and V2…….. 17*

*Figure 1.12: Source gather straight lines representation, velocity through a layer is the inverse of the gradient of the times plotted with distance.…….. 18*

*Figure 1.13: A source gather from the problematic area of the 3D seismic survey showing velocity inversion…….. 20*

*Figure 1.14: Single Layer velocity model averages many velocities (from surface to datum) in the near surface…….. 21*

*Figure 1.15: Earth model velocity Inversion: note the head-waves illustrating the longer travel path for the ray passing through the velocity inversion…….. 22*

*Figure 1.16: Source gather gradients of the times plotted with distance representing the earth model in figure 1.15…….. 23*

*Figure 1.17: Elevation profile showing the thickness of the shallow layer and changes in deeper refractor velocities …….. 24*

*Figure 1.18: Source gather from a 3D seismic survey showing a major cycle skip…….. 25*

*Figure 1.19: Earth model source gather with cycle skip caused by velocity inversion of figure 1.18..... 26*

*Figure 1.20: Refractor complexities example, Time disruption dues to refractor breaks, create data cycle skips..... 28*

*Figure 2.1: Test 3D data Low frequency statics, from left to right: Low frequency statics of the single-layer model, low frequency statics of the multi-layer model and the difference between them..... 33*

*Figure 3.1: A shot record from the static problem zone. No statics applied..... 38*

*Figure 3.2: The same shot record from the static problem zone. The arrow indicates a cycle skip developed after applying conventional statics solution (high frequency multi-layer model) ..... 39*

*Figure 3.3: Cross-line (A) stack with the high frequency statics of the single layer model and the internal pilot residual statics. Conventional residual statics improved the stack response with no data breaks..... 40*

*Figure 3.4: Cross-line (A) stack with the high frequency statics of the multi-layer model and the internal pilot residual statics. Conventional residual statics exaggerated data breaks to cycle skips..... 41*

*Figure 3.5: In-line (B) stack with the high frequency statics of the single layer model and the internal pilot residual statics. Conventional residual statics improved the stack response with no data breaks..... 42*

*Figure 3.6: In-line (B) stack with the high frequency statics of the multi-layer model and the internal pilot residual statics. Conventional residual statics induced data discontinuity..... 43*

*Figure 3.7: A schematic chart of the proposed approach to fix statics cycle skips..... 46*

*Figure 3.8: Post-stack data conditioning..... 47*

*Figure 4.1: The example source gather after applying new methodology statics solution..... 50*

*Figure 4.2: Part of cross-line (A) stack with the new approach statics solution (top), and the conventional approach statics solution (bottom) ..... 51*

*Figure 4.3: Post-stack volume time slice at 700 ms in the XY direction. New statics solution (top) and old statics solution (bottom). Arrows indicate to places where data had cycle skips..... 52*

*Figure 4.4: Post-stack volume time slice at 1400 ms in the XY direction. New statics solution (top) and old statics solution (bottom). Arrows indicate to places where data had cycle skips..... 53*

*Figure 4.5: Full seismic section in the cross-line direction (cross-line B).New statics solution resulted in reasonable data continuity with no cycle skips…….. 54*

*Figure 4.6: Full seismic section in the inline direction (inline A). New statics solution resulted in reasonable data continuity with no cycle skips…….. 55*

## ملخص الرسالة

الكسور الغير حقيقية في البيانات السيزمية في العادة لا يمكن معالجتها بالطرق الستاتيكية العادية. مثل هذه الكسور تعطي نتائج مضللة في التفسيرات الاستكشافية الجيوفيزيائية أو الجيولوجية و قد تعطي صورة غير حقيقية للتراكيب التحت سطحية. عند تطبيق التصحيح الستاتيكي المبني علي طريقة الطبقة الواحدة أو الطبقات المتعددة هناك كسور غير حقيقية قد تنشأ عن ذلك. بالرغم من أن الطرق العادية لتصحيح ما تحمله البيانات السيزمية من بقايا ستاتيكية في العادة قادرة على معالجة مثل هذه المشاكل الا انها فشلت في معالجة حالات عديدة. في هذه الدراسة قمت بتصحيح مثل هذه الكسور عن طريق تصميم طريقة جديدة. هذه الطريقة الجديدة مبنية على بناء نموذج مشتق من البيانات السيزمية ذاتها و تطبيق نوعي التصحيحات الستاتيكية من نموذجين ستاتيكيين مختلفين لتكوين نموذج خليط باستخدام استاتيكيات التردد العالي المأخوذة من نموذج استاتيكي محسوب بطريقة الطبقة الواحدة مع استاتيكيات التردد المنخفض العالي المأخوذة من نموذج استاتيكي محسوب بطريقة الطبقات المتعددة.الطريقة الجديدة هذه تم اختبارها على مشروع ثلاثي الابعاد لبيانات سيزمية تم تسجيلها بمنطقة حقل الحبا بالمنطقة الشرقية للملكة العربية السعودية حيث تم معاجة كسر غير حقيقي كبير في الطبقات التحت سطحية و الناشيء عن تطبيق الحل الستاتيكي المحسوب بطريقة الطبقات المتعددة. النتائج النهائية كانت جيدة جدا و أعطت صورة اكثر واقعية للطبقات التحت سطحية.

# THESIS ABSTRACT

Name: Emad Ekladios Toma Tawadros
Title: Resolving the Cycle Skip Introduced by the Multi-Layer Static Model using a Hybrid Approach
Major Field: Geophysics
Date: June 2011

Cycle skips (breaks) in seismic data are occasionally irresolvable using conventional static correction programs. Such artificial cycle skips can be misleading for interpreters and introduce false subsurface images. After applying datum static corrections using either the single-layer or multi-layer models, artificial cycle skips might develop in the data. Although conventional residual static correction techniques are occasionally able to solve this problem, they fail in solving many other cases.

A new approach is introduced in this study to resolve this problem by forming a static model that is free of these artificial cycle skips, which can be used as a pilot volume for residual statics calculation. The pilot volume is formed by combining the high-frequency static component of the single-layer model which show better static solution at the static problem locations and the low-frequency static component of the two-layer model. This new approach is applied on a 3-D seismic data set from Haba Field of Eastern Saudi Arabia where a major cycle skip was introduced by the multi-layer model. Results show a better image of the subsurface structure after application of the new approach.

Master of Science Degree
King Fahd University of Petroleum and Minerals
Dhahran, Saudi Arabia
June 2011

# CHAPTER 1

# INTRODUCTION

## 1.1 Introduction

Interpreters strive for the delineation of more accurate and subsurface images. Artificial cycle skips can be generated in seismic data by one or more processing steps, which can be misleading because they introduce nonrealistic subsurface images (Butler et al., 2005; Buck et al., 1996; Bridle et al., 2005). Although many static correction techniques can be used to resolve many of these artificial cycle skips, in some cases, none of the conventional residual static techniques can resolve them. The new technique proposed here provides a tool that hybridizes the high-frequency static component of the single-layer static model with the low-frequency static component of the multi-layer static model, as shown in Figure 1.1. This static combination is used to form a smooth data-driven stack model that can be used as an external pilot to correct the cycle skips in the data.

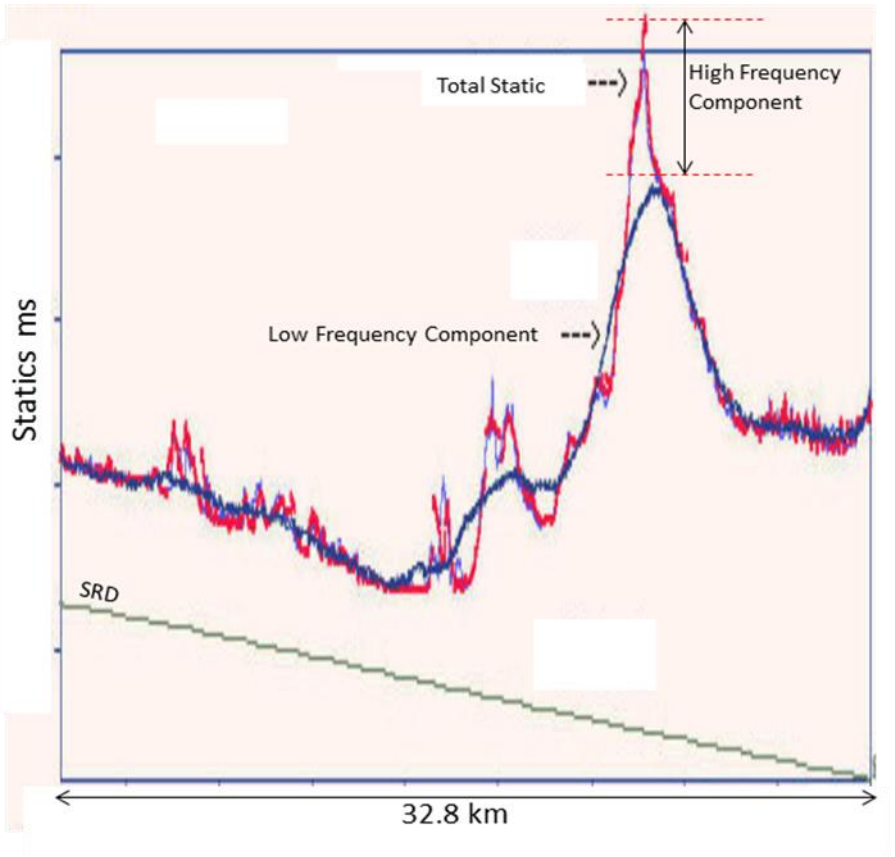


*Figure 1.1: Partitioning of total statics. The red curve represents the high-frequency component taken from the single-layer model whereas the blue curve represents the low-frequency static component taken from the two-layer model. The greenish line represents the seismic reference datum (SRD).*

This thesis is organized in five chapters. Chapter 1 gives the background of the problem and states its causes. Chapter 2 describes the objective of the thesis. Chapter 3 describes the methodology that has been followed in this thesis to solve the problem. Chapter 4 presents the results of the tests. Finally, Chapter 5 concludes with the main findings of the thesis.

## 1.2 Problem Statement

In more than 90% of the seismic projects in Saudi Arabia, the multi-layer model has generated a better static solution than the single-layer model. However, in some seismic projects, the application of multi-layer velocity model statics has generated breaks (cycle skips) in the data (Danborn et al., 2005; Zhang et al., 2005; Ley II et al., 2003). Conventional residual statics methods are often unsuccessful in resolving these model-induced cycle skips. I applied my approach to a 3D seismic data set acquired over the Haba field in Eastern Saudi Arabia.

Figure 1.2 shows the aerial extension of the study's 3D seismic data with an in-line (B) and a cross-line (A) passing through the static problem zone. The problem can be shown from post-stack data and pre-stack data. Figure 1.3 is a time slice through the post-stack volume, which shows clearly that the conventional method of multi-layer statics failed to fix a data break that

developed cycle skips. Figures 1.4 and 1.5 show the cross-line (A) with the high frequency statics component of the single-layer and multi-layer models, respectively. The multi-layer statics introduced data breaks whereas the single-layer statics showed reasonable data continuity. Figures 1.6 and 1.7 show the in-line (B) with the high frequency statics component of the single-layer and multi-layer models, respectively. The data break in the in-line direction is not as clear as that in the cross-line direction. However, the single-layer high frequency statics model produces better stack continuity than the multi-layer high frequency statics do. Figure 1.8 presents a shot record from the problem zone where the application of the multi-layer high frequency statics component introduced a clear cycle skip.

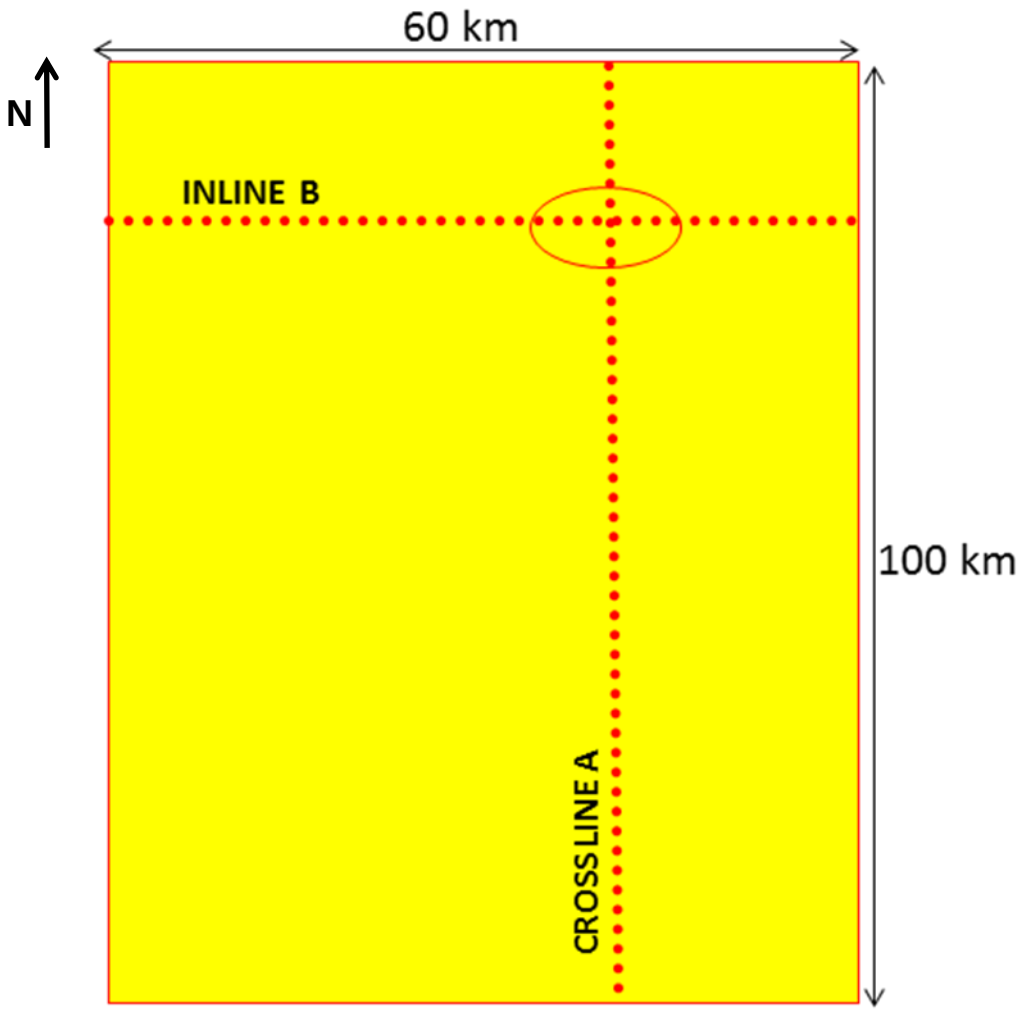


*Figure 1.2: Aerial dimensions of 3D area under study. Oval shape indicates the cycle skip problem area.*

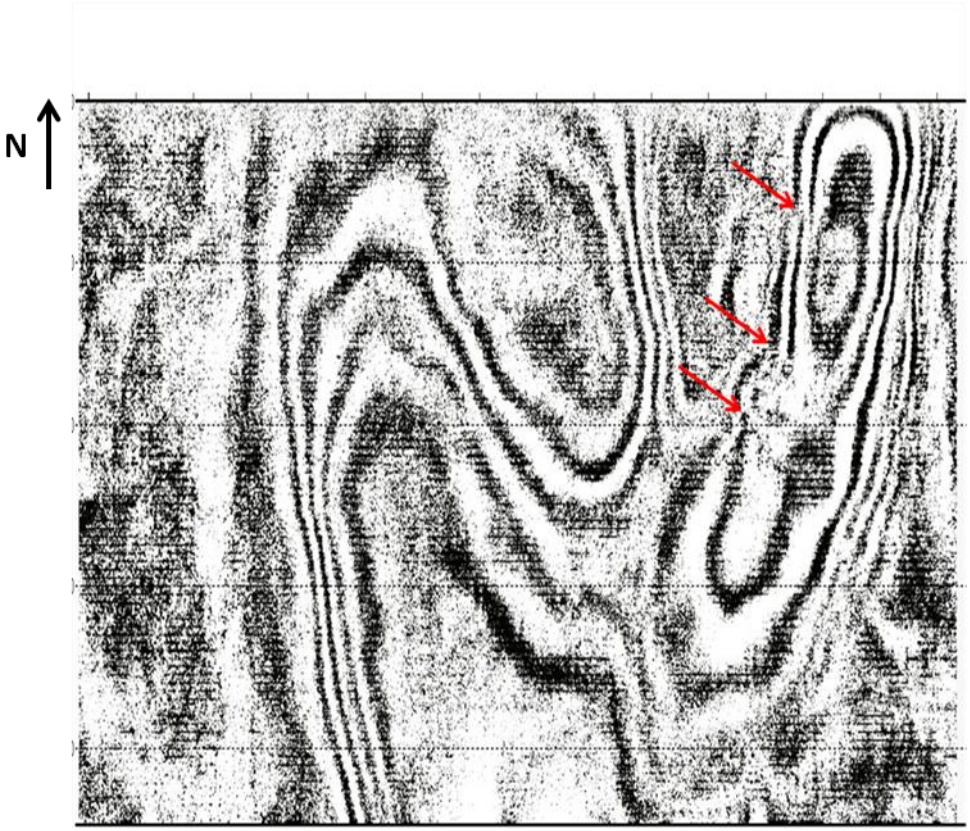


*Figure 1.3: Time slice at 1400 ms, conventional static solution (multi-layer model and internal pilot residual statics applied). The arrows indicate the clear cycle skips introduced.*

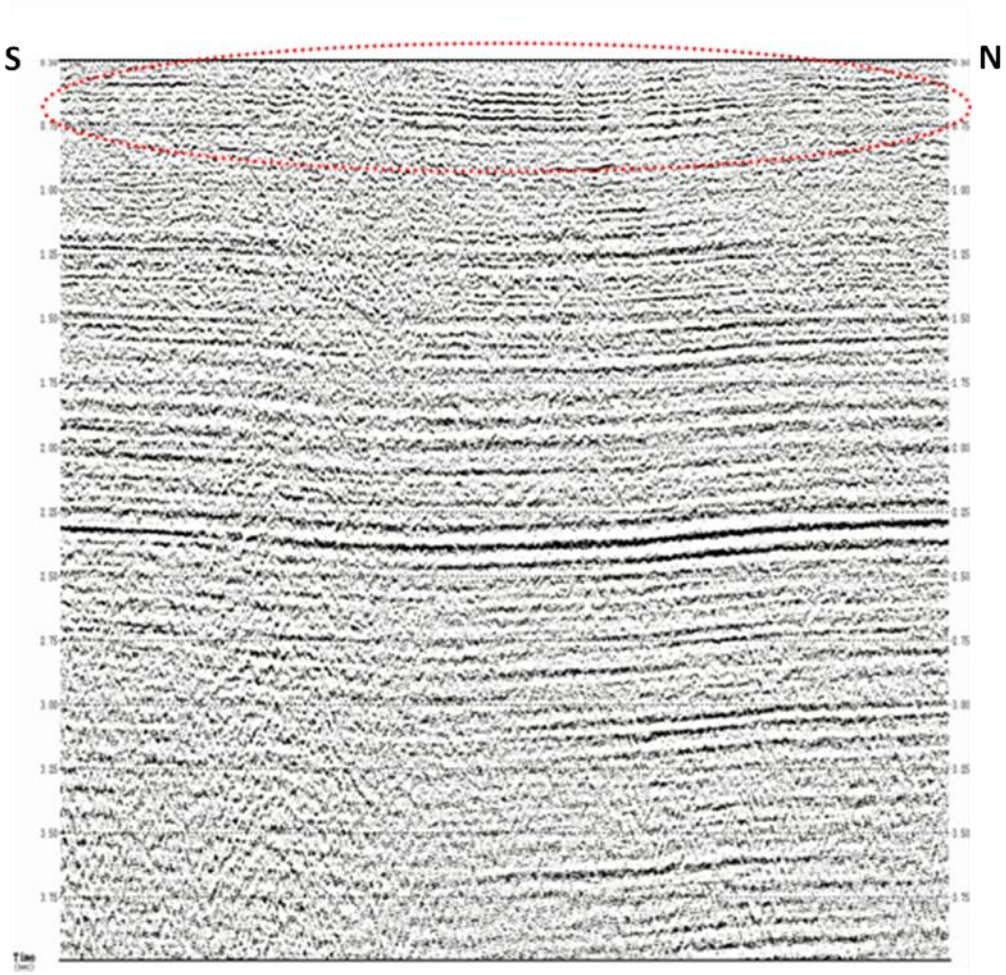


*Figure 1.4: Cross-line (A) stack with the high frequency statics of the single-layer model. Note the reasonable data continuity within the dashed line.*

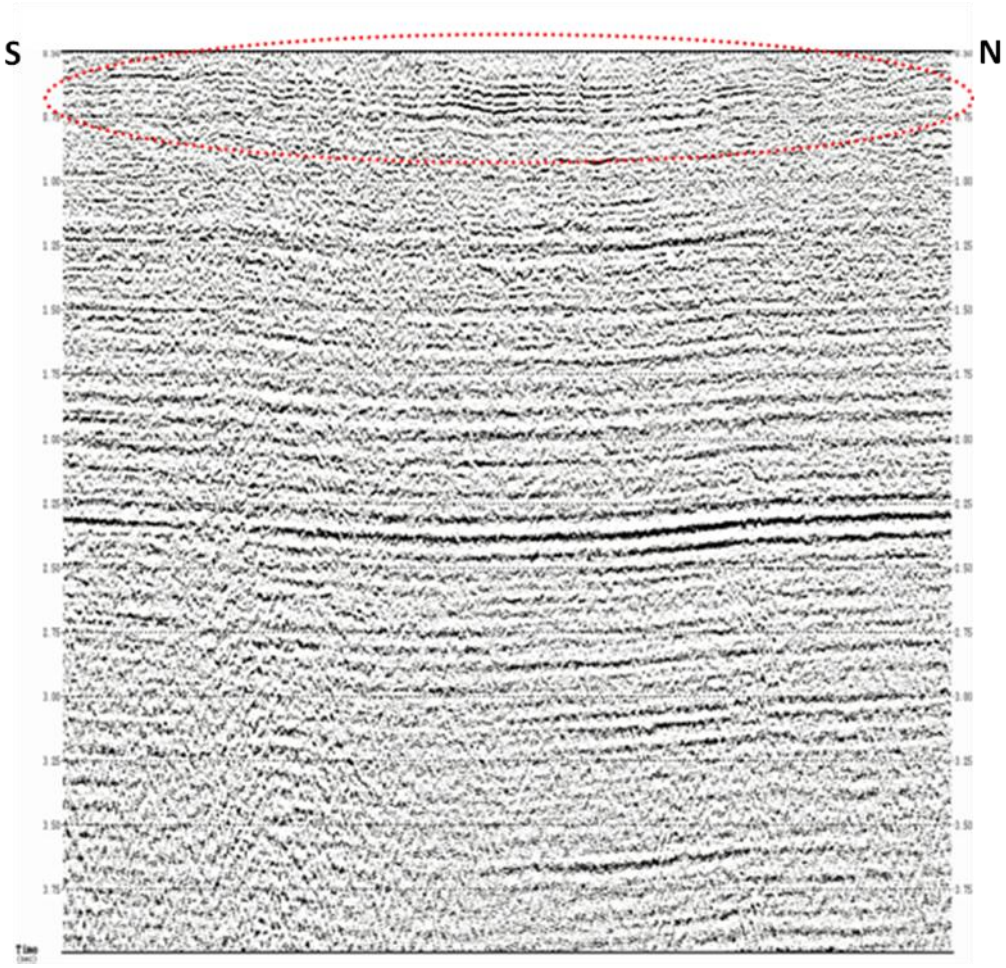


*Figure 1.5: Cross-line (A) stack with the high frequency statics of the multi-layer model. Note the data continuity breaks within the dashed line.*

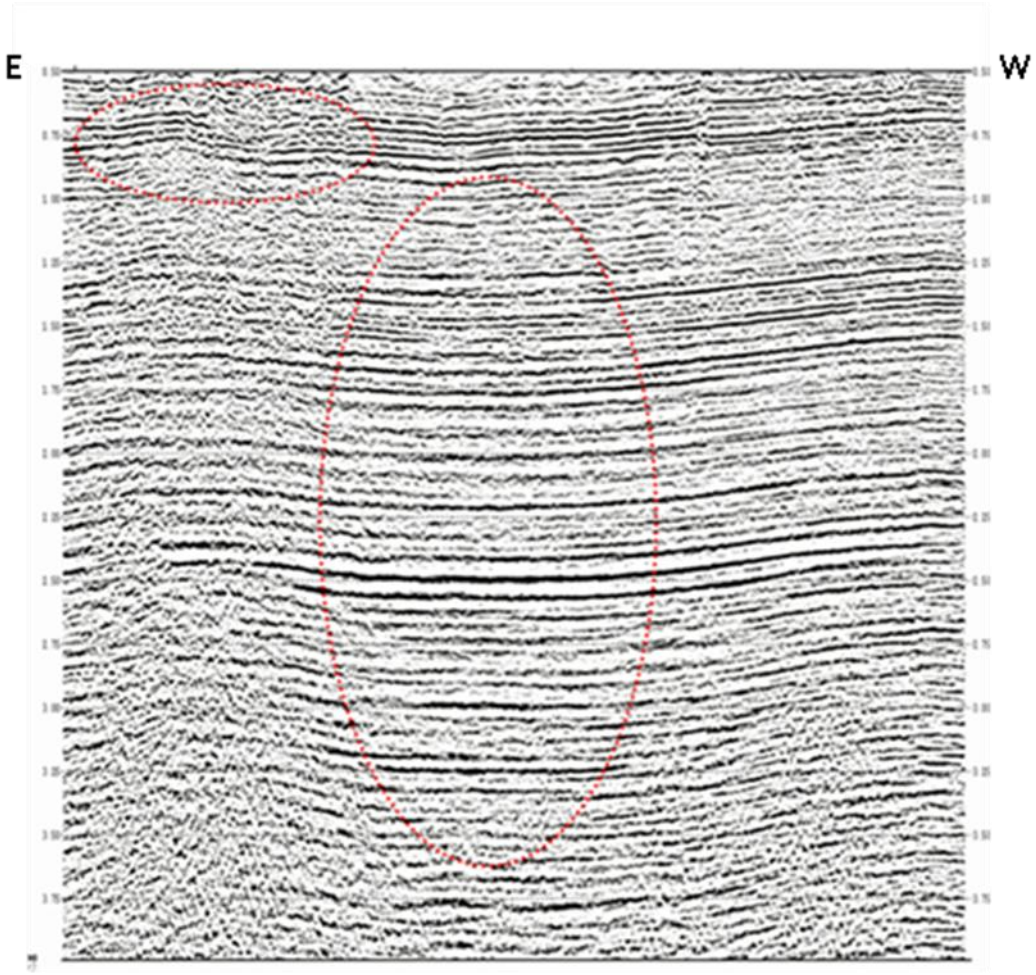


*Figure 1.6: In-line (B) stack with the high frequency statics of the single-layer model.*
*Note the reasonable data continuity within the dashed line.*

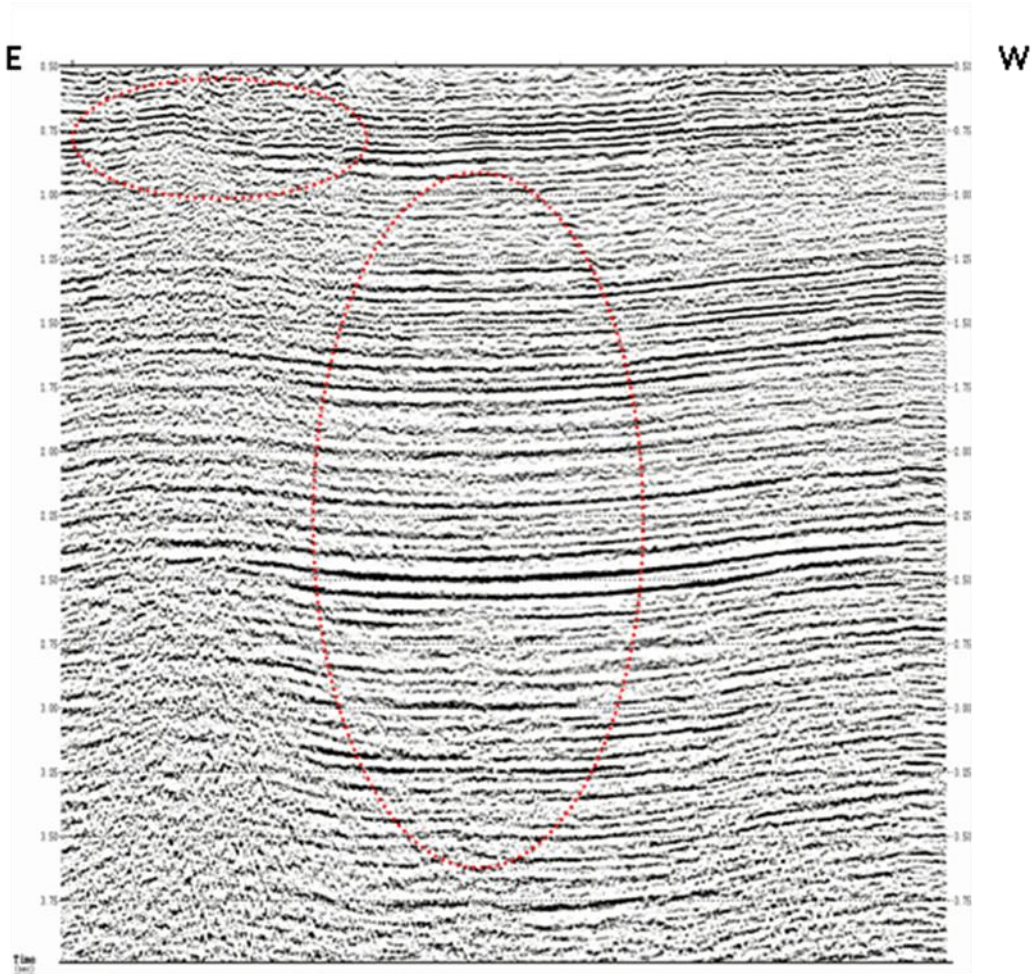


*Figure 1.7: In-line (B) stack with the high frequency statics of the multi-layer model. Note that data breaks are not as clear as those on the cross-line.*

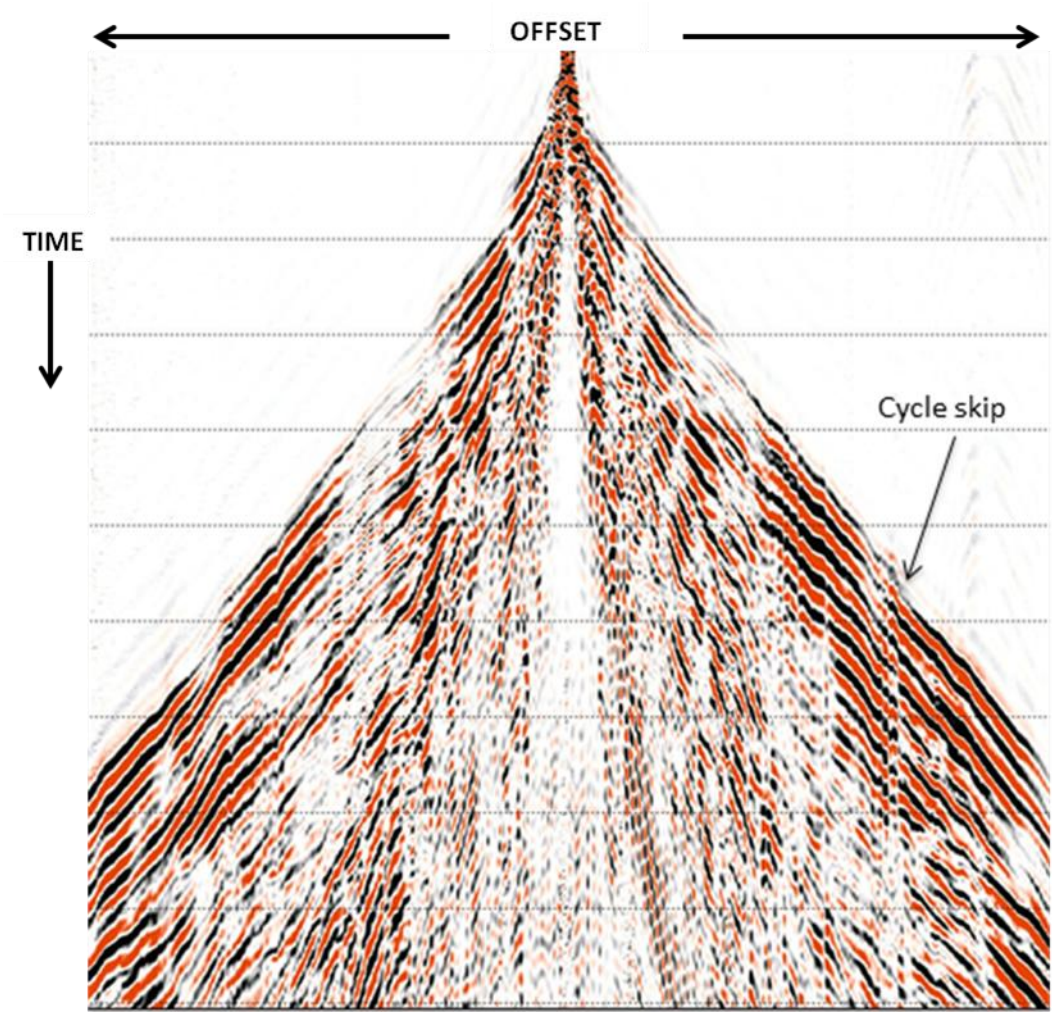


*Figure 1.8: An example shot record, conventional static solution (multi-layer applied). The arrow indicates a clear cycle skip introduced.*

## 1.3 The Cause

The application of single-layer velocity model statics to our data showed a skip-free result compared with the multi-layer velocity model statics. The main cause of the cycle skip is that the multi-layer model uses horizontal ray paths, which are mainly recorded from refracted energy (Palmer et al., 1986) whereas the single-layer model uses near vertical ray paths that are recorded in upholes from direct arrivals. The refracting-ray geometry for two horizontal interfaces is shown in Figure 1.9 where two rays travel from a source location to two receivers on a flat surface. Figure 1.10 shows an uphole recording vertical or near vertical travel paths.

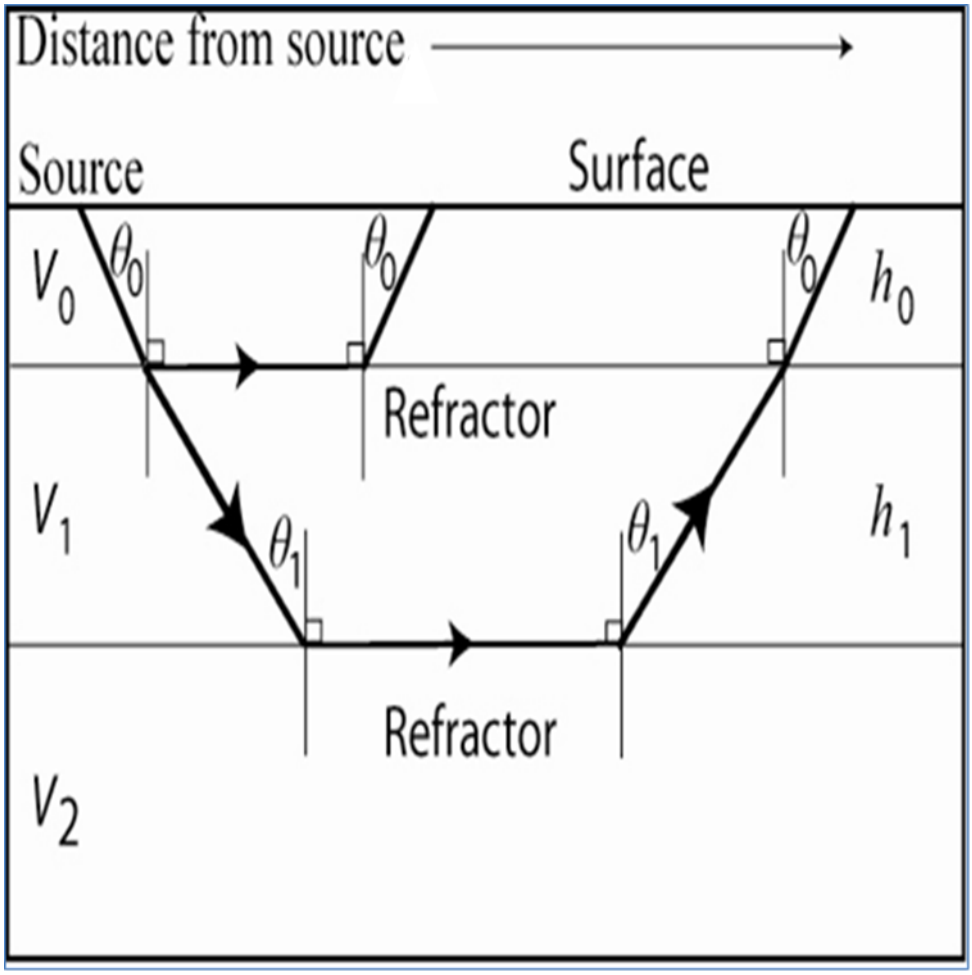


*Figure 1.9: Earth model, two ray paths travelling just below refractors at velocities of V1 and V2*

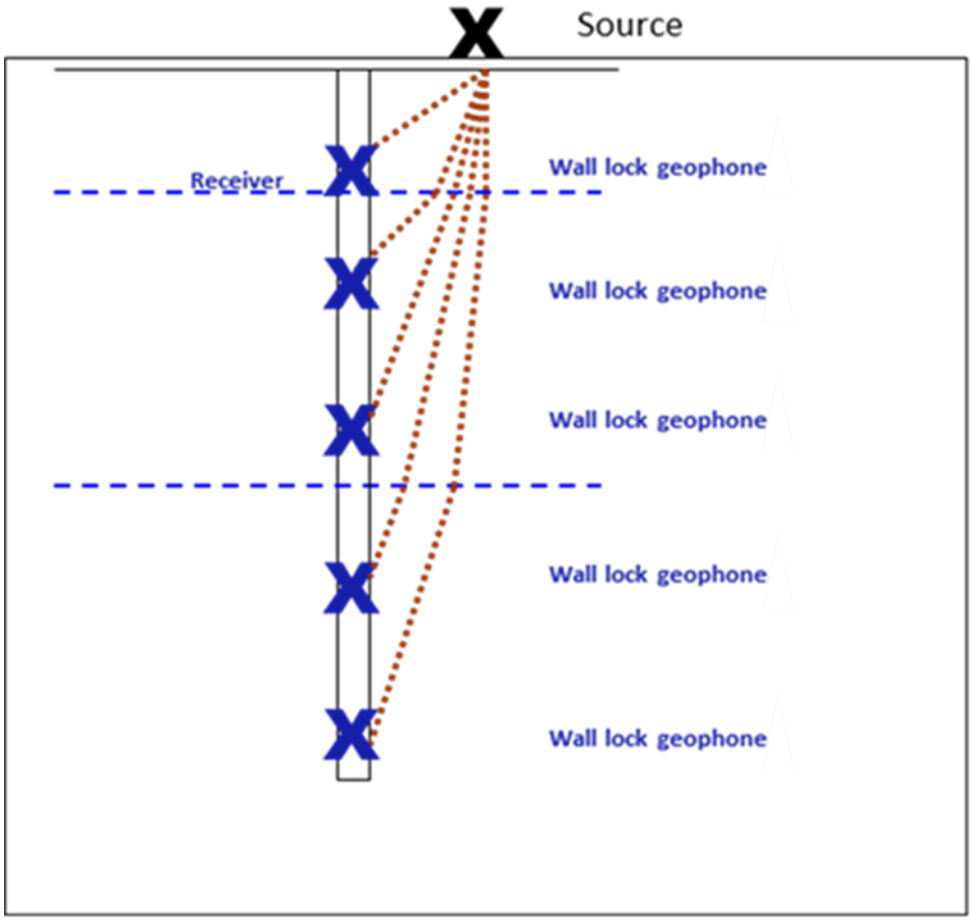


*Figure 1.10: An uphole recording near vertical ray paths (Sheriff, 2002).*

Many problems are associated with horizontal ray paths, such as the cases of buried anomalies, velocity inversions, and complex refractors.

### 1.3.1. Buried anomalies

Buried anomalies can be shallow (Figure 1.11), so they will be unseen by the refracted traces. On the other hand, if an uphole passes this anomaly, it will affect the velocity recorded by that uphole; otherwise, it will be unseen by the uphole as well. Problems occur in some areas because the refractor velocity assigned to a certain location on the surface in fact comes from a spread that is relatively far from that location. As a result, any detectable anomaly in the near surface under that spread will affect the velocity at that location. In other words, the multi-layer velocity model image shows detectable shallow anomalies laterally away from its real location. This effect occurs because a shallow anomaly produces an extra amount of time added to or subtracted from the static delay time and is seen only on the near traces (small offsets); whereas the far traces (larger offsets) do not experience the shallow anomaly. When statics are applied, they shift the traces erroneously at the unrealistic anomaly location, which leads to a vertical break or a static cycle skip. In the case of the single-layer velocity model, when an anomaly is located in between upholes, it will be unseen by the uphole. This effect occurs because the uphole records near vertical traces (Figure 1.10). Because the single-layer velocity model statics are calculated by interpolation

of the average velocities from the upholes, no extra time shifts affect the statics values and, consequently, no data breaks occur. Figure 1.12 shows the diagram of a source gather with the straight lines representing the first arrivals, which ignore small anomalies beneath the source and/or the receiver.

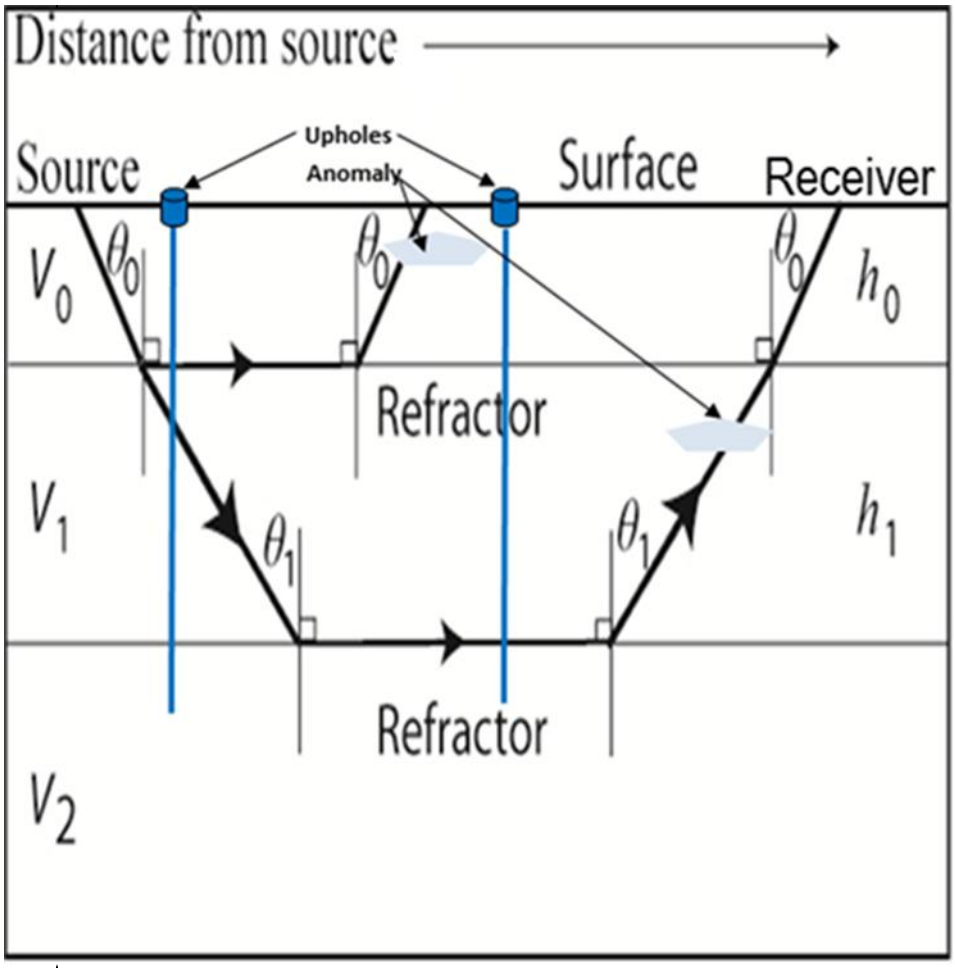


*Figure 1.11: Buried anomalies: two ray paths travelling just below refractors at velocities of V1 and V2. An anomaly in layer 1 may only be detected by the shallow ray path (near offset trace) refracted off the first interface whereas the deeper refracted energy (far offset trace) may only detect deeper or farther anomalies.*

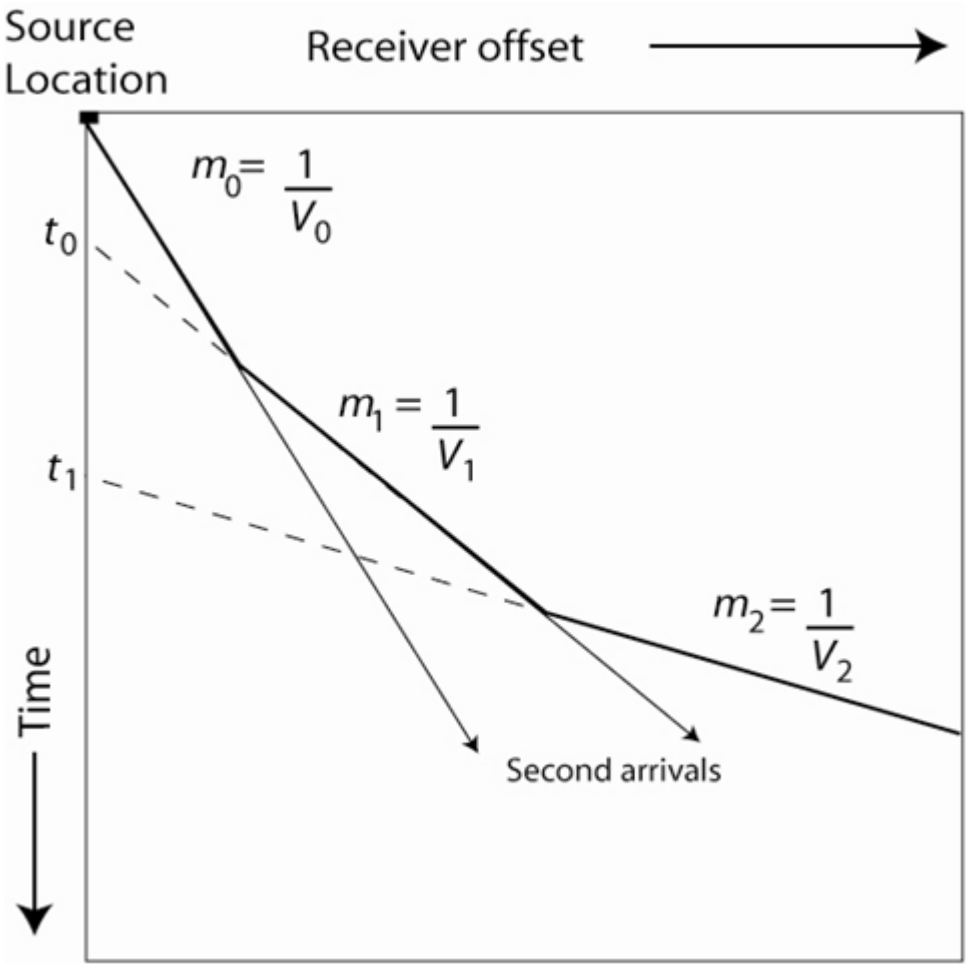


*Figure 1.12: A source gather straight lines representation; velocity through a layer is the inverse of the gradient of the times plotted with distance. Anomalies do not affect the velocity gradients (Sheriff, 2002).*

### 1.3.2. Velocity inversion

The existence of velocity inversions has been recognized as a challenge in defining the near surface in head-wave analysis (Knox, 1967). By analyzing source records around the problematic area, a shot record located in the data break area showed a typical refractor velocity inversion. Part of the refractor exists on the near traces only and disappears at the far traces, as shown in Figure 1.13. The single-layer velocity model ignores the velocity inversion as it is based on upholes that record vertical or near-vertical traces. It averages velocities to represent the near surface, as shown in Figure 1.14.

The multi-layer velocity model (intercept time method) produces an extra intercept time because of the decrease of velocity with depth, consequently creating an invisible layer as represented by the earth model shown in Figure 1.15 and the diagram of the source gather shown in Figure 1.16. Unlike the single-layer velocity model, the multi-layer velocity model always honors the weathering and sub-weathering layers (Figure 1.17). A source gather and its earth model of a real data example showing a cycle skip caused by velocity inversion are shown in Figures 1.18 and 1.19, respectively (Bridle, 2008).

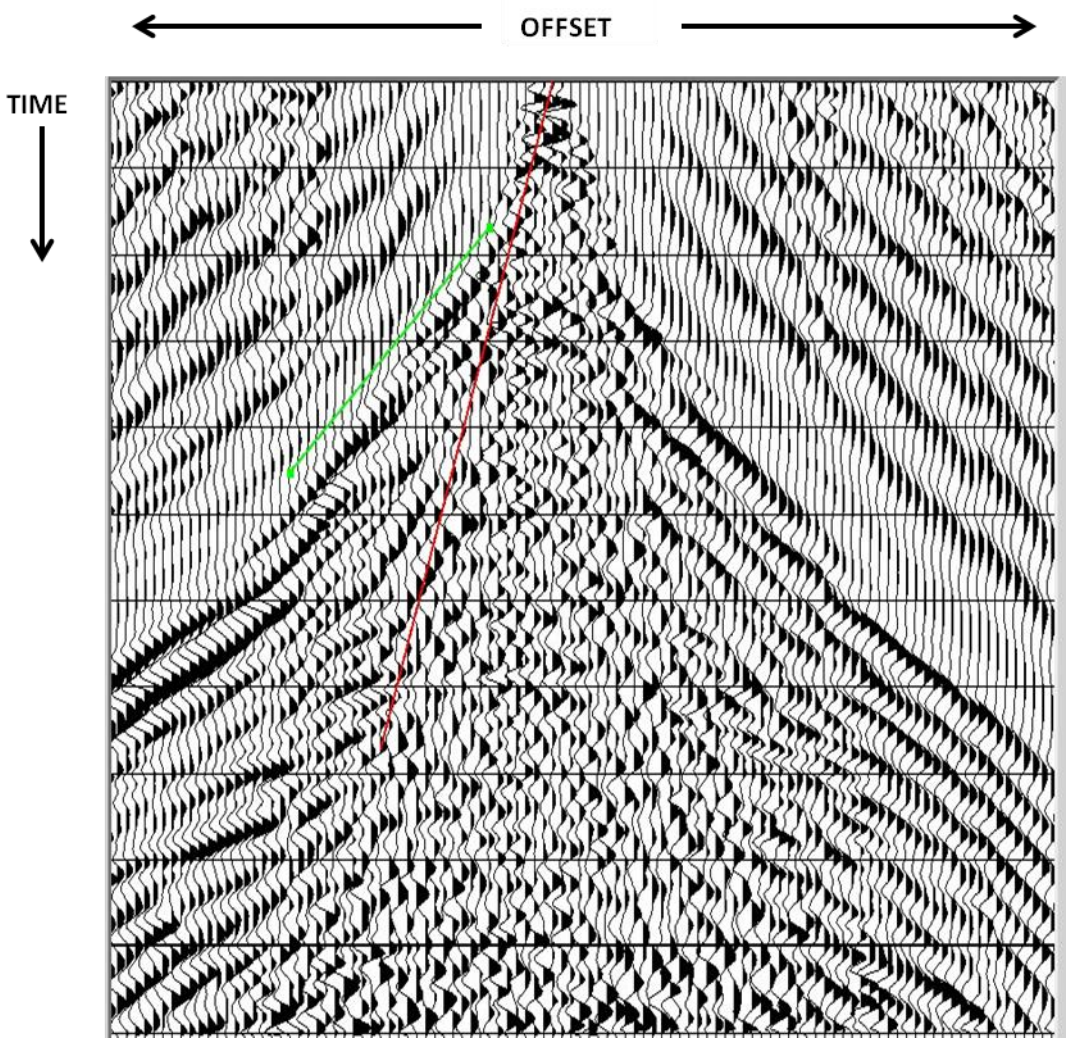


*Figure 1.13: A source gather from the problematic area of the 3D seismic survey showing velocity inversion. Note that part of the refractor exists only on the near-offset traces and disappears at the far-offset traces.*

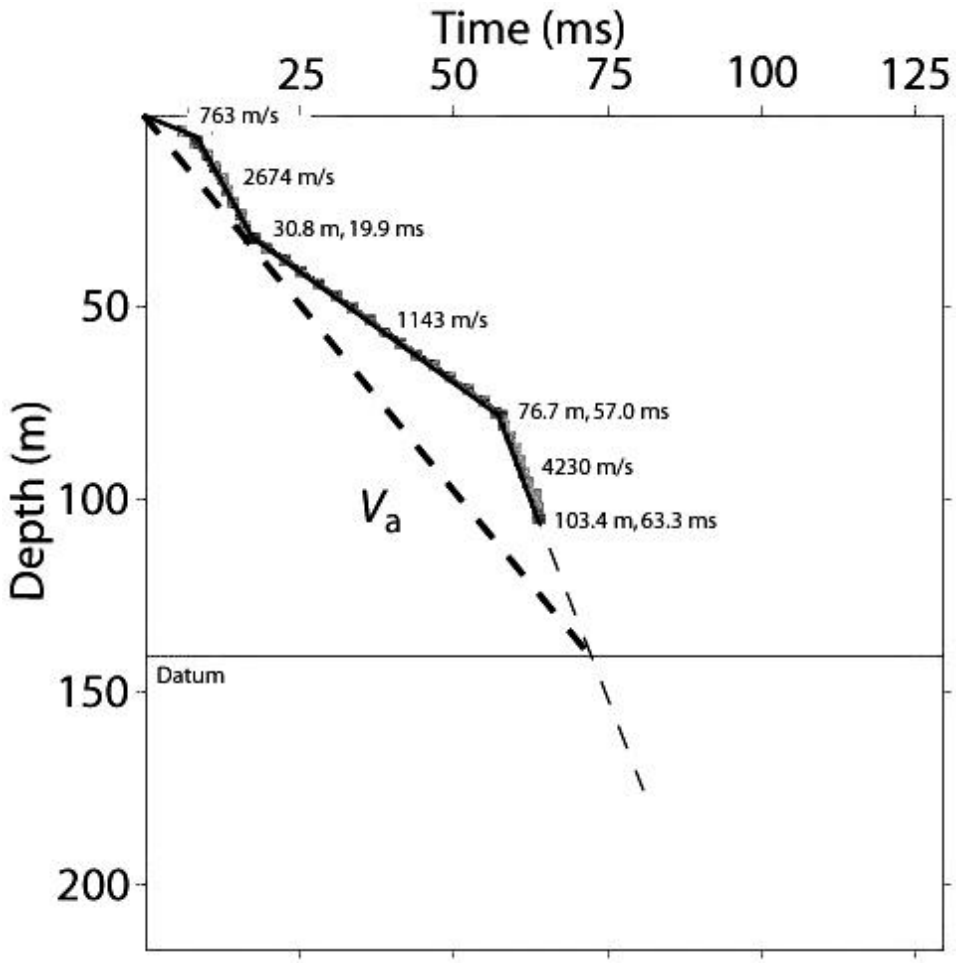


*Figure 1.14: Single-layer velocity model averages many velocities (from surface to datum) in the near surface. Weathering and sub-weathering faster velocities are averaged.*

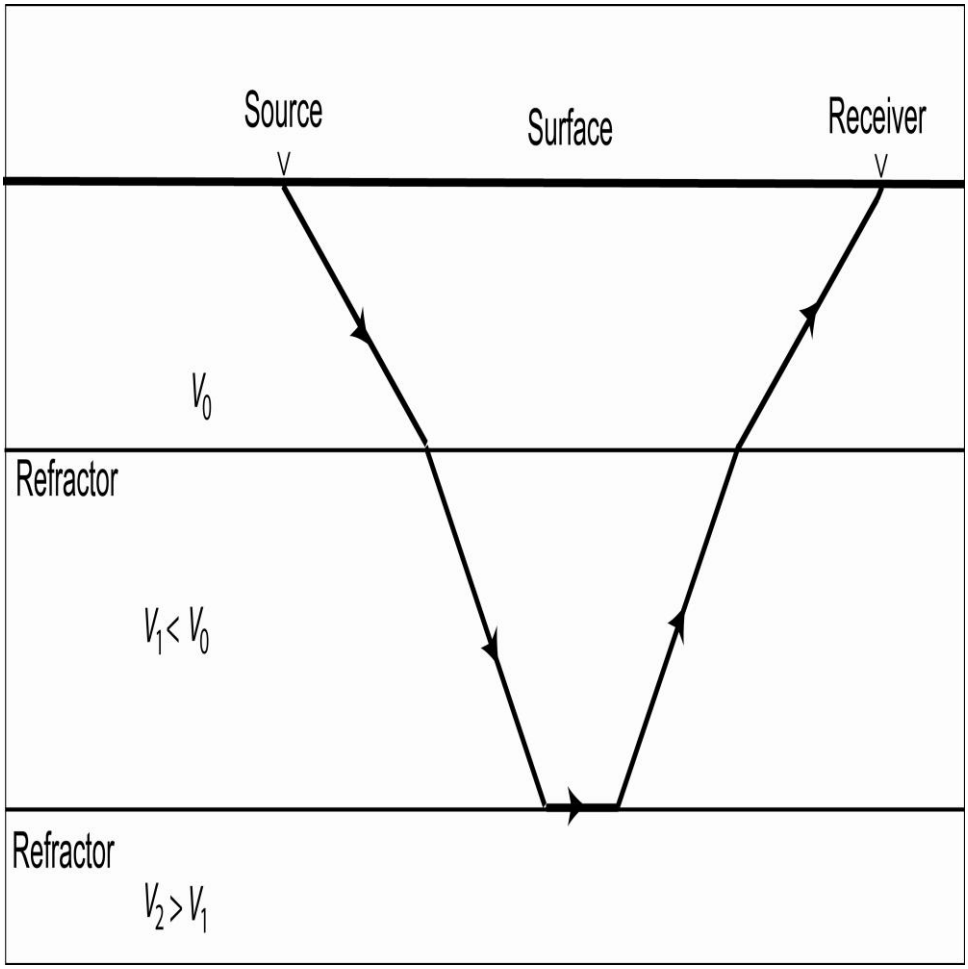


*Figure 1.15: Earth model showing velocity inversion: note the head-waves illustrating the longer travel path for the ray passing through the velocity inversion. Extra time will be added to the refracted wave causing the time delay represented in Figure 1.14 by the slow velocity of 1143 m/s.*

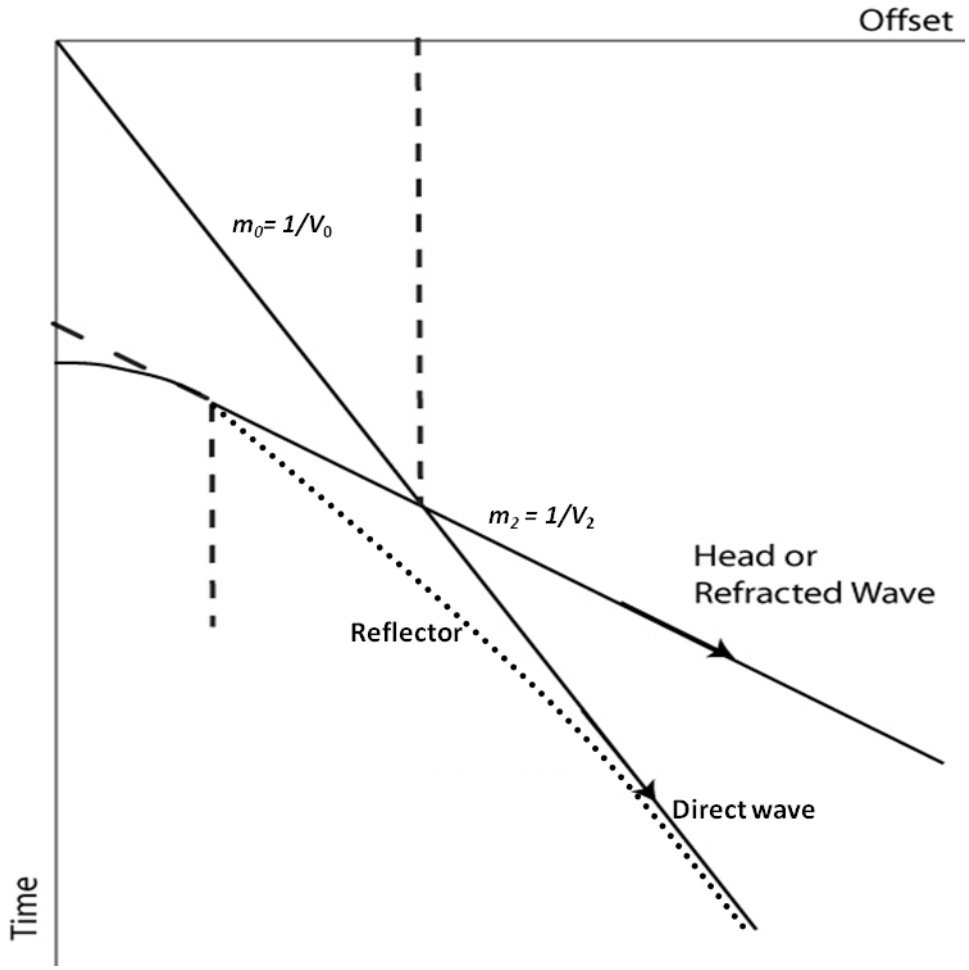


*Figure 1.16: Source gather gradients of the times plotted with distance representing the earth model in Figure 1.15. Note that layer 1 that has the velocity inversion is invisible on the record.*

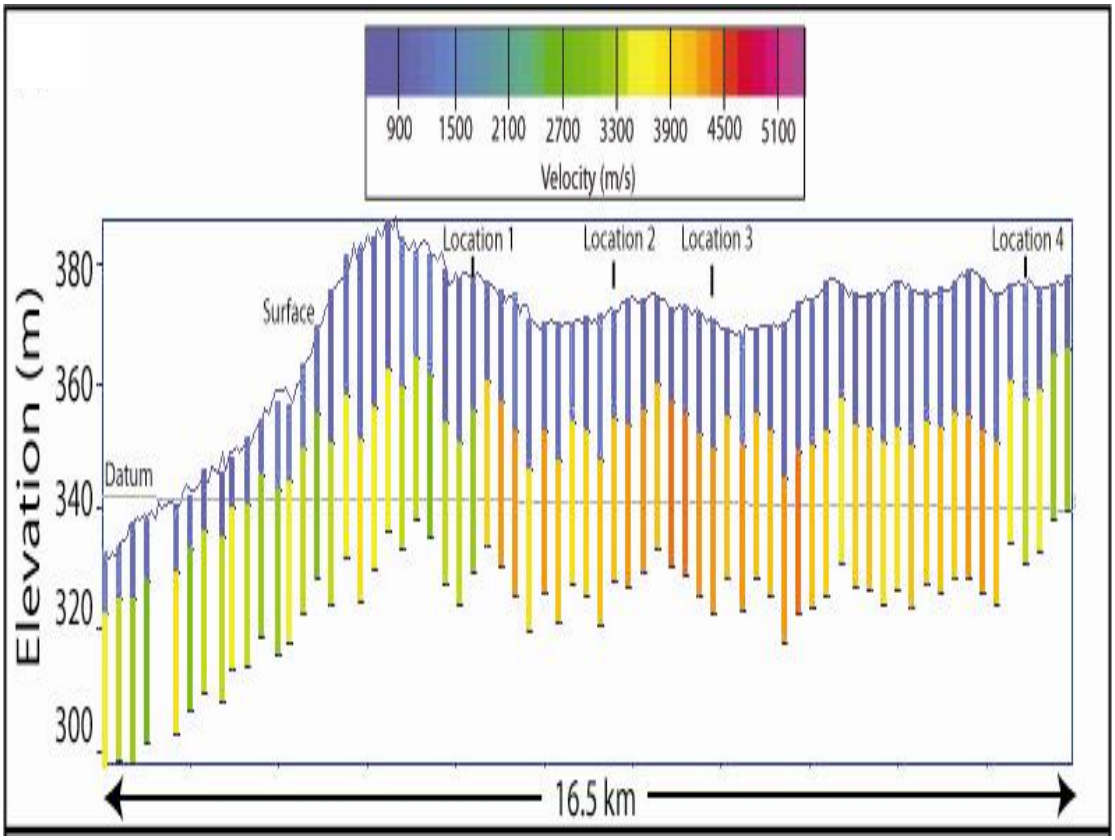


*Figure 1.17: Elevation profile along a seismic line showing the thickness of the shallow layer and changes in deeper refractor velocities.*

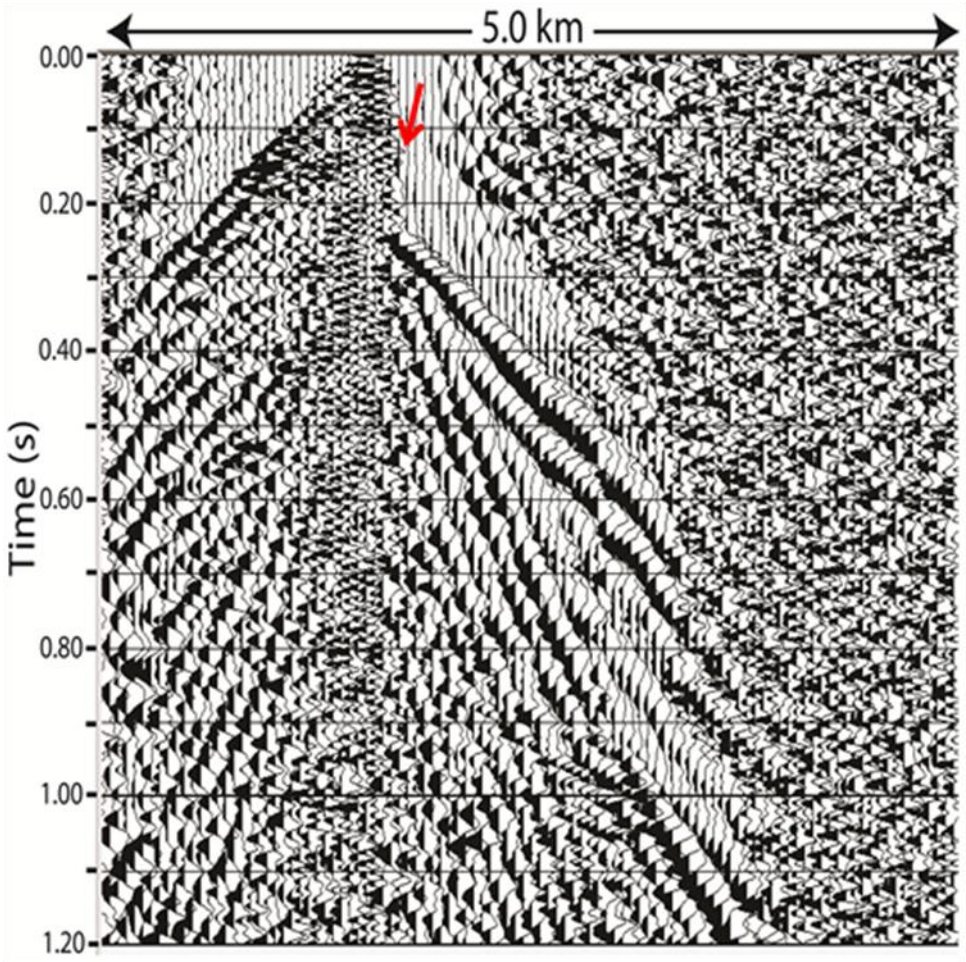


*Figure 1.18: Source gather from a 3D seismic survey showing a major cycle skip caused by a velocity inversion, indicated by the arrow*

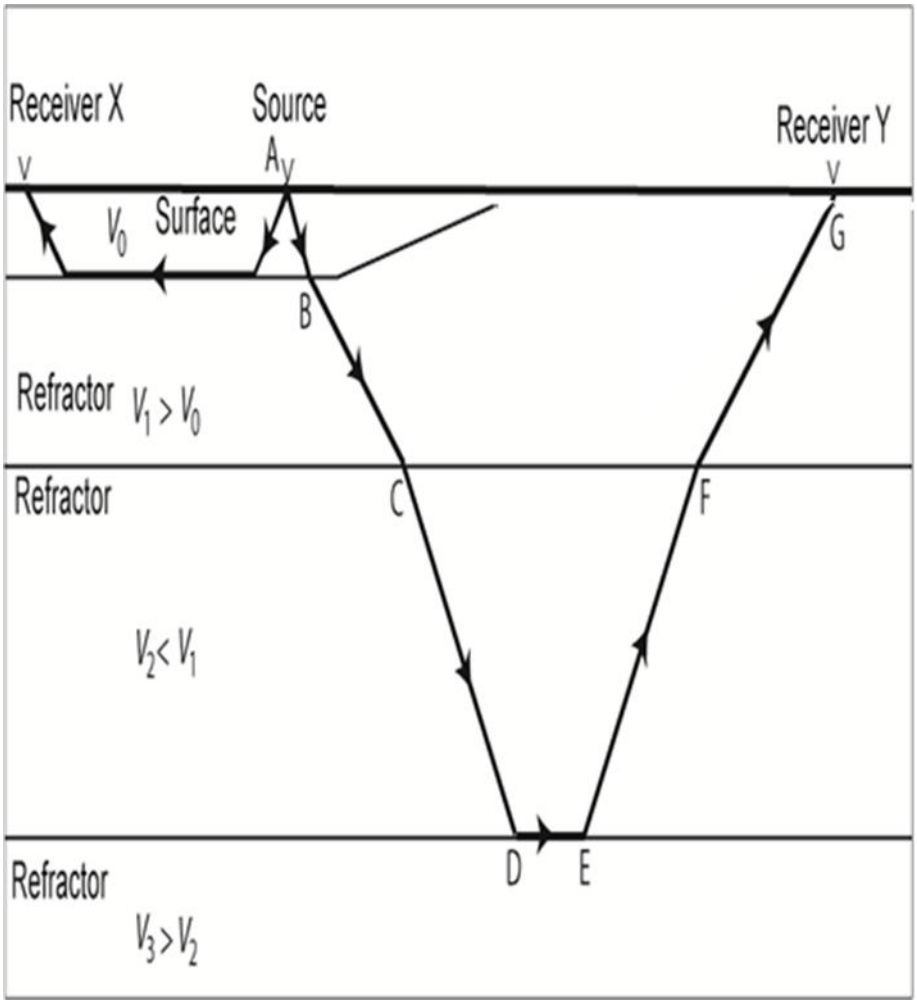


*Figure 1.19: Earth model source gather with a cycle skip caused by the velocity inversion shown in Figure 1.18. The transmitted ray path on the pinch outside travels a much longer path because of the velocity inversion.*

### 1.3.3. Complex refractors

In the case of the multi-layer model, the discontinuity of a refractor causes time delays or advances, which may lead to cycle skips. In the case of the single-layer model, the vertical ray recorded in an uphole will not experience the horizontal refractor discontinuity (Bridle et al., 2009; Cox et al., 1999; Cunningham et al., 1974; Hatherly et al., 1994). Figure 1.20 shows a typical discontinuous refractor; in this case, cycle skips are probable.

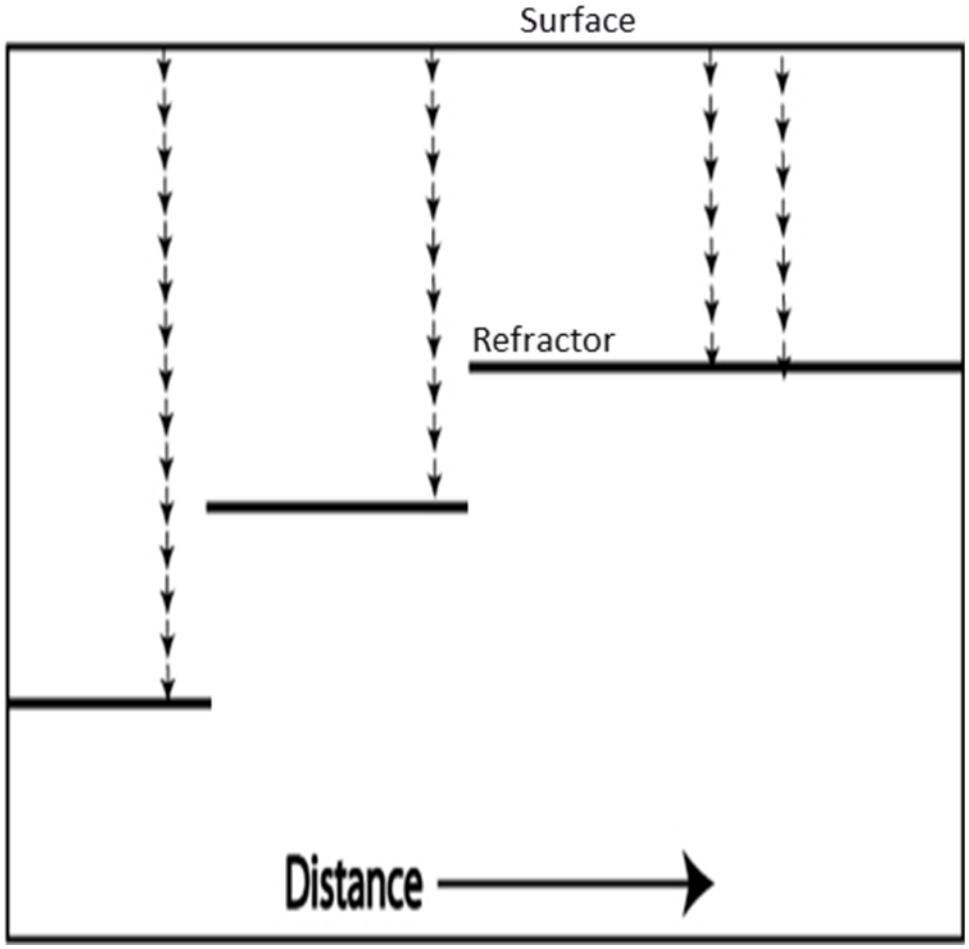


*Figure 1.20: Example of refractor complexities. Time disruption due to refractor breaks creates data cycle skips.*

# CHAPTER 2

# OBJECTIVE

## 2.1 Introduction

In the seismic processing world, the total datum static correction that is applied to data is divided into two components. The first is called the high frequency static component, and the second is called the low frequency static component (Yilmaz, 1987). As shown in Figure1.1, the red curve representing the shot and receiver elevation equivalents in milliseconds is smoothed. The difference between the smooth surface and the original surface is the high frequency static component. The difference between the smooth surface and the seismic reference datum (SRD) is the low frequency static component. The high frequency static component is applied to the pre-stack gathers before the application of the normal moveout (NMO) correction. High frequency static components are relative statics between traces in pre-stack gathers. The goal of their application is to align pre-stack traces relatively before the NMO application in order to obtain the best stack response of those traces. The low frequency static component is applied in a later stage after NMO correction. This static component is applied to reference the data from the smooth surface to the seismic reference datum. As explained in Chapter 1, possible causes of cycle skips are concerned with the high frequency static component.

## 2.2 Concept

The application of the high frequency static component of the single-layer model resulted in skip-free data (Figure 1.4) compared with the result of the application of the high frequency static component of the multi-layer model (Figure 1.5). Therefore, our objective is to use the high frequency static component from the single-layer model for pre-NMO static correction and the low frequency static component from the multi-layer model for post-NMO static correction. One may ask the question of why we do not use both the high and the low frequency components from the multi-layer static model. The answer to this question is that the majority of Saudi Arabian seismic projects use the high and low frequency static components of the more realistic multi-layer static model. Application of these static components has resulted in better data continuity and stack response than the results of the single-layer static model stack. Kingdom-wide minor data showed better data continuity when applying static components from the single-layer model than the continuity when applying static components of the multi-layer model. Thus, we have to use the high frequency static components from the single-layer model and the low frequency static components from the multi-layer model. If we use the low frequency static components from the single-layer model for a minor data zone that has a static cycle skip, other kinds of artificial static mismatch between data with multi-layer low frequency static components and data with the single-layer model low frequency static components will arise.

Figure 2.1 shows the magnitude of the difference between the multi-layer and the single-layer low frequency statics in our 3D project under study. It is clear that the difference is appreciable and that it ranges from -11 to +120 ms. Because of this large static difference and the fact that the multi-layer static model was applied on all surrounding seismic projects to ensure static consistency of the whole survey, we have to apply the low frequency static component from the multi-layer model. In particular, cycle skips occurred only on limited zones (see the oval dashed area in Figure 2.1) of the study's 3D project. Furthermore, to make the final total statics applied to our project, including the static break zone, homogenous and consistent with other surrounding seismic projects, we utilize the residual static technique in a non-conventional way in order to fix the cycle skip introduced by the multi-layer model. In other words, our final data result will show the multi-layer high and low frequency statics applied as for any multi-layer static model application for datum static correction, with the residual statics computed especially to fix the cycle skips.

Therefore, our objective is to compute residual statics that can efficiently repair cycle skips that are irresolvable using conventional techniques. Common conventional techniques include single-layer or multi-layer static model computation and conventional residual static computation. What is special about the residual statics computation proposed in the new methodology is the use of an external pilot that is built by applying the high frequency statics from the single-layer model to the input pre-stack gathers

and applying the low frequency statics from the multi-layer model to the post-stack data volume (Yilmaz, 1987).

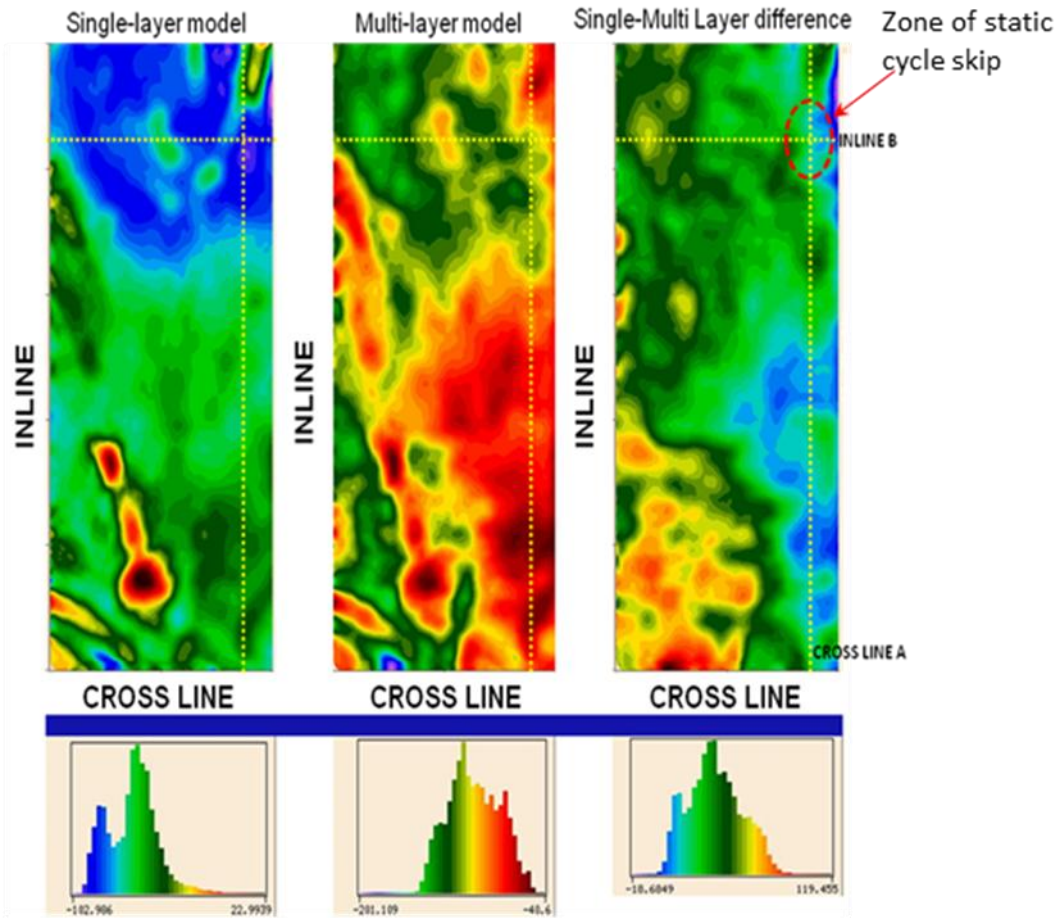


*Figure 2.1: Test 3D data low frequency statics. From left to right: low frequency statics of the single-layer model, low frequency statics of the multi-layer model, and the difference between them. The bottom part shows histograms of the statics value ranges in ms, which are 124, 240 and 130 ms, respectively.*

## 2.3 Data processing

Input data must be pre-processed pre-stack for residual statics computation and then pre-conditioned post-stack for external pilot generation. The following steps are the processing sequence that is applied pre-stack to prepare the data for residual statics computation and application:

1. Transcription from SEGD field tape to the processing software format
2. Noise attenuation of 50/60 Hz sinusoidal power lines
3. Geometric spreading compensation
4. Multi-layer datum static correction (i.e., applying the high frequency statics)
5. First pass of 3km by 3km velocity analysis
6. Strong energy noise attenuation and 3D linear noise attenuation
7. First pass of surface-consistent amplitude scaling
8. First pass of surface-consistent deconvolution
9. Second pass of surface-consistent amplitude scaling

The post-stack processing sequence, which is applied after the external pilot generation, is very important because it improves the signal-to-noise ratio and smoothes the data to make sure that the input data-driven external pilot is free from any artificial static breaks. The sequence of this process is as follows:

1. Surface-consistent residual statics

2. Second pass of velocity analysis

3. Stacking

4. Automatic gain control with a gate length of 1000 ms

5. Multi-layer datum static correction (i.e., applying the low frequency statics)

Examples of the data after the pre- and post-stack sequences are shown in Chapter 3.

# CHAPTER 3

# METHODOLOGY

## 3.1 Introduction

A 3D seismic data set was chosen in which conventional residual statics techniques failed to resolve cycle skips introduced by the multi-layer velocity model statics. This chapter describes the conventional methodology used for resolving the data breaks introduced by the multi-layer model in addition to the methodology proposed to resolve the static problem. The chapter describes some attempts using conventional methodology to resolve the data break, including static application results of both the pre-stack and post-stack data. The results of the proposed methodology for pre-stack data and post-stack data are also presented.

## 3.2 Conventional Methodology

The conventional methodology attempts to solve the problem using conventional statics techniques. Figures 3.1 and 3.2, respectively, show the pre-stack data with no statics applied. The application of the high frequency component from the multi-layer model induced a cycle skip rather than fixing the static break. In Chapter 1, we saw how the post-stack data was reasonably continuous when the high frequency of the single-layer model

was applied (cross-line in Figure 1.4 and in-line in Figure 1.6). We also saw how the multi-layer static model introduced a data break (cross-line in Figure 1.5 and in-line in Figure 1.7). Here, Figures 3.3 and 3.4 show results of the application of the high frequency datum statics and the internal pilot residual statics for the single-layer statics and the multi-layer statics models, respectively. Note that conventional residual statics computed on top of the multi-layer model developed a cycle skip. Similarly, Figures 3.5 and 3.6 show the results for the in-line direction. Note that the static break in the in-line direction is not as clear as shown in the cross line direction. In other words, the cross-line data shows a clear cycle skip whereas the in-line data shows only a discontinuity.

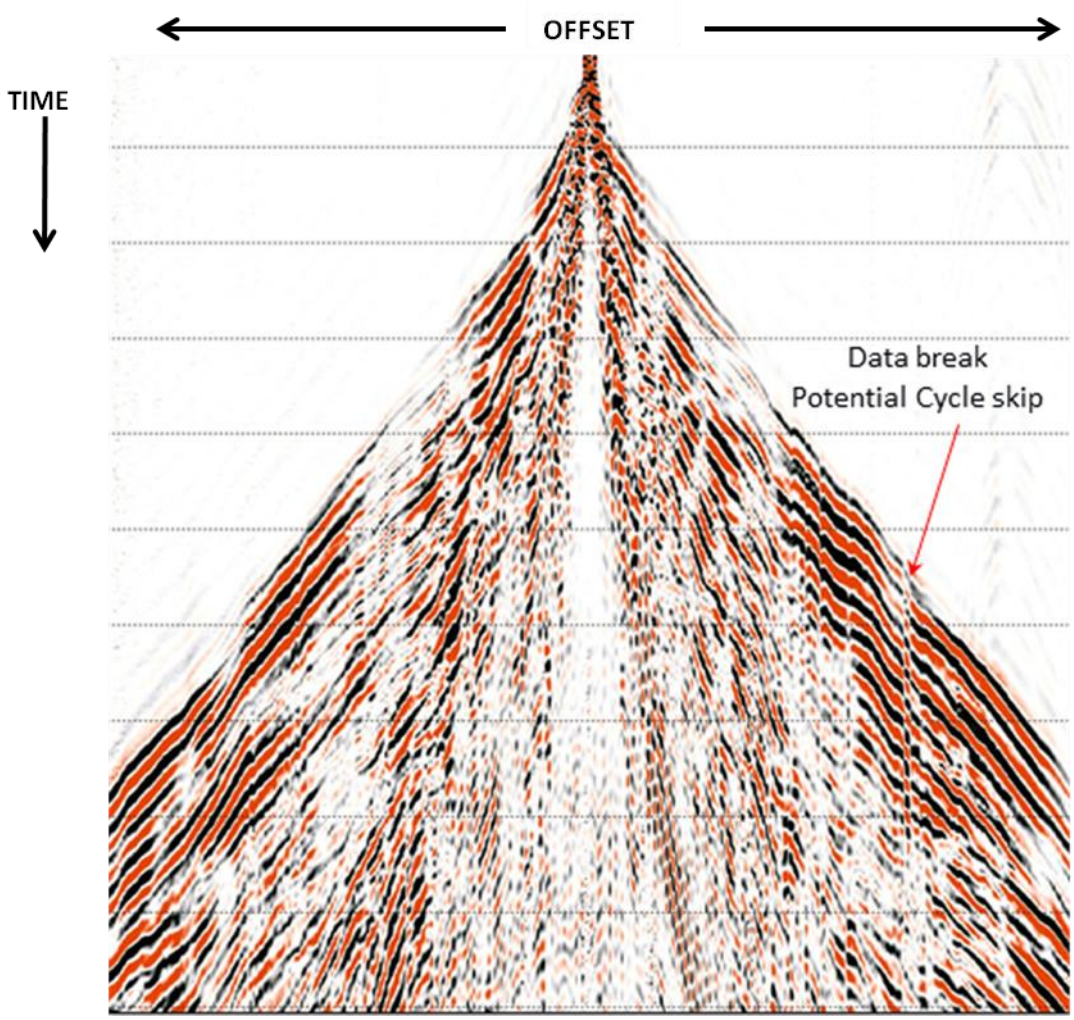


*Figure 3.1: A shot record from the static problem zone. With no statics applied, the arrow indicates a static data break that is irresolvable using conventional statics techniques.*

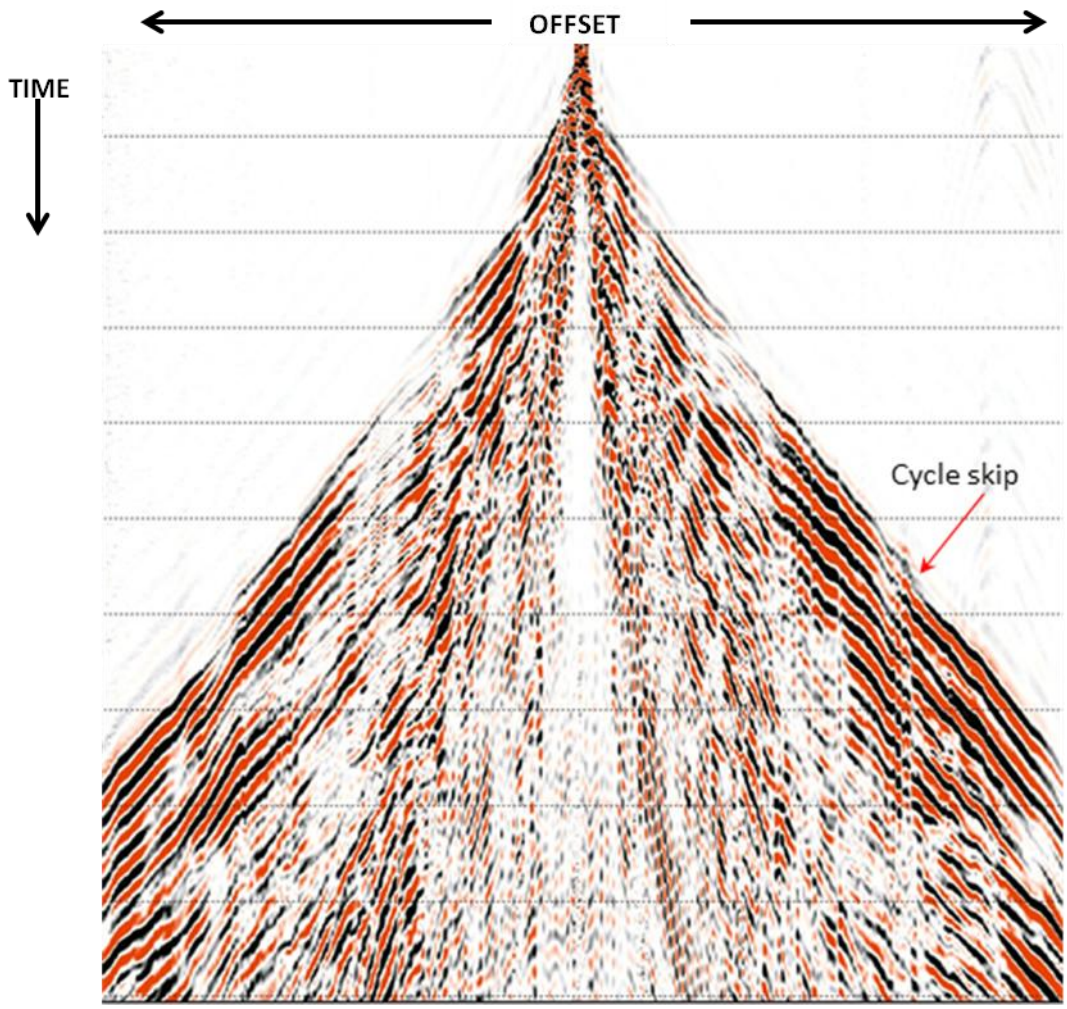


*Figure 3.2: The same shot record from the static problem zone. The arrow indicates a cycle skip developed after applying a conventional statics solution (high frequency multi-layer model).*

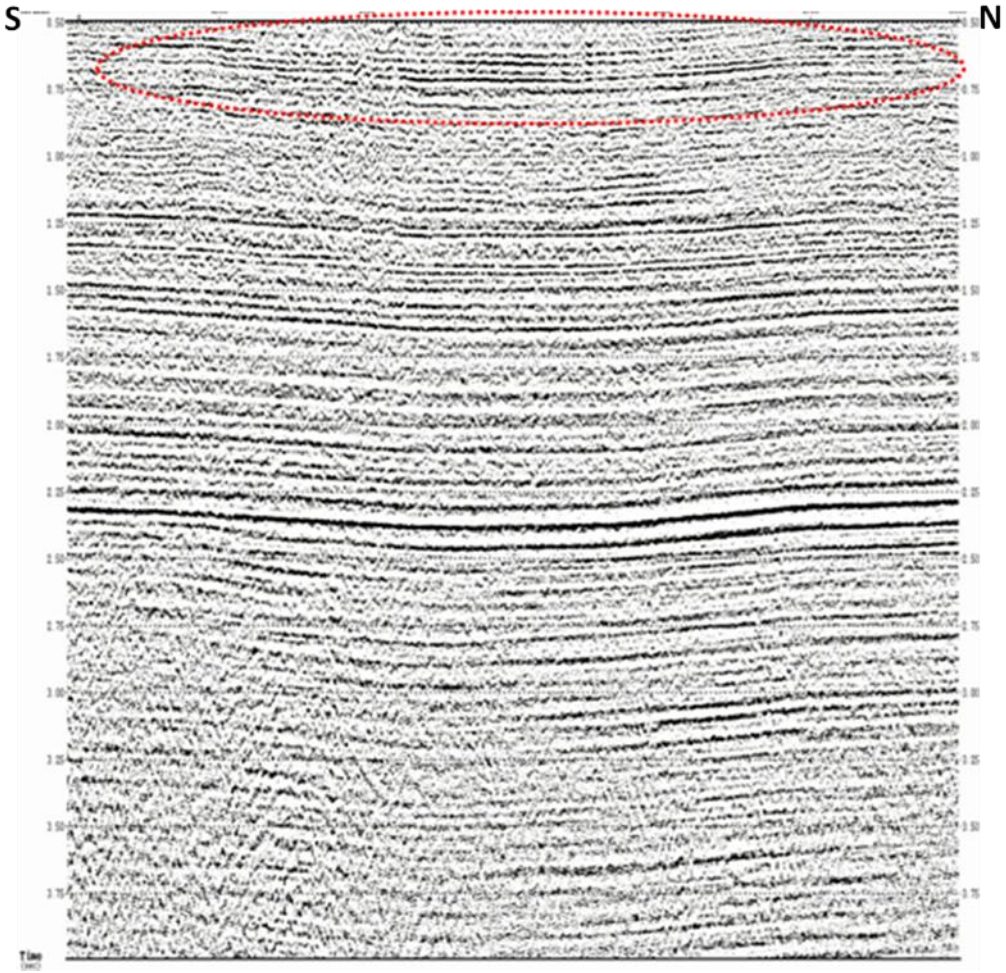


*Figure 3.3: Cross-line (A) stack with the high frequency statics of the single-layer model and the internal pilot residual statics. Conventional residual statics improved the stack response with no data breaks.*

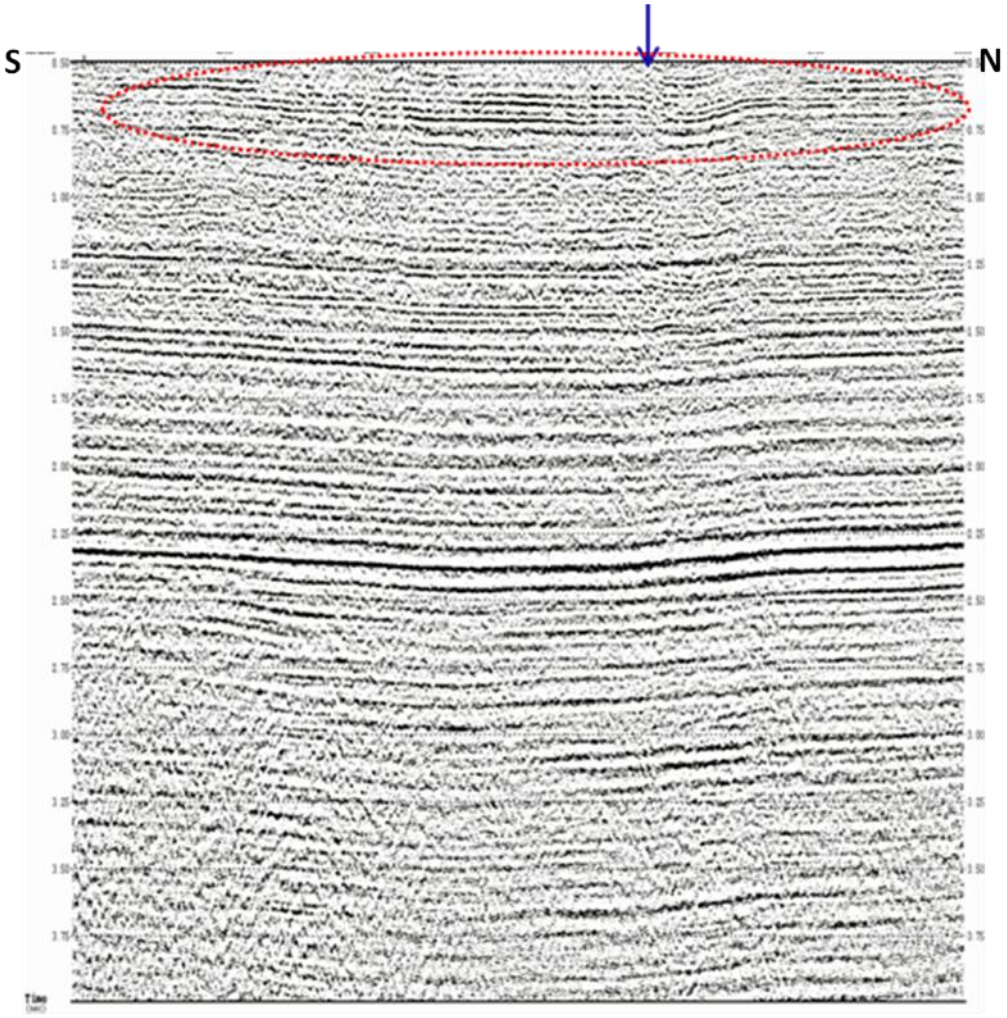


*Figure 3.4: Cross-line (A) stack with the high frequency statics of the multi-layer model and the internal pilot residual statics. Conventional residual statics exaggerated data breaks to cycle skips (indicated by the arrow).*

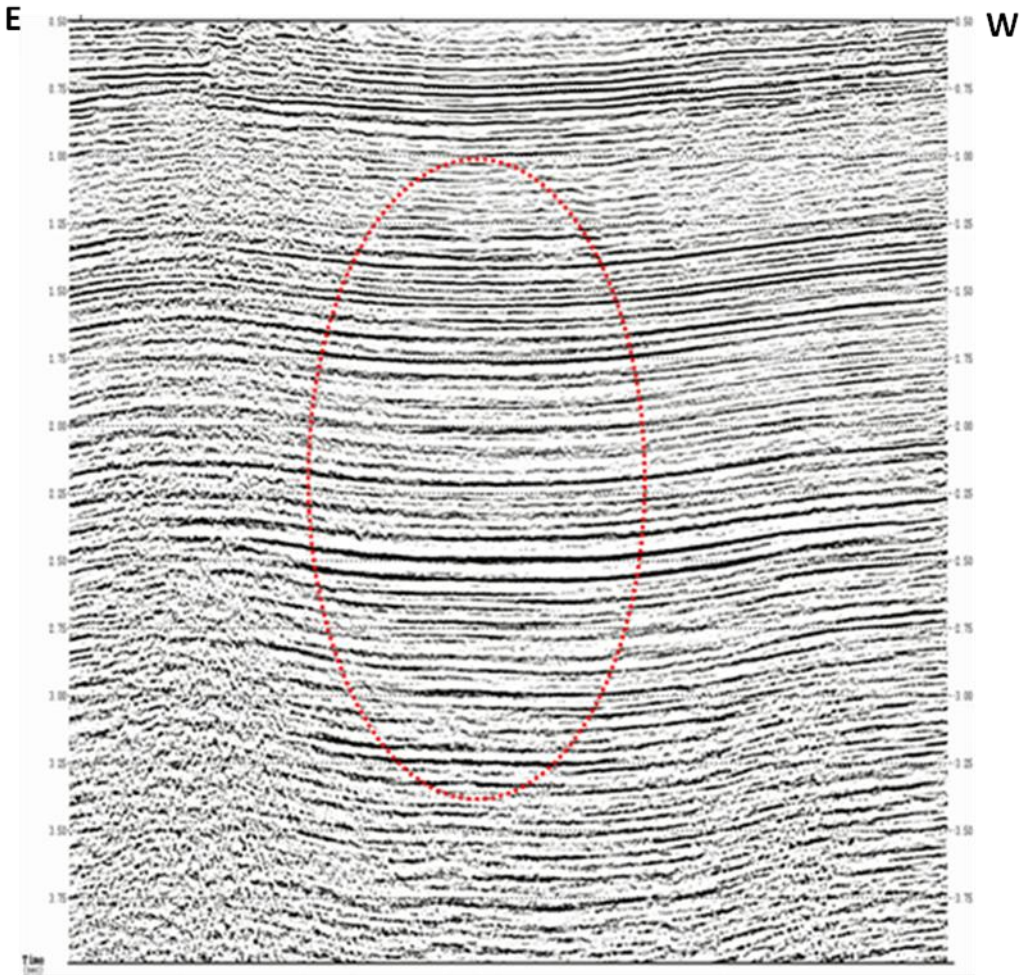


*Figure 3.5: In-line (B) stack with the high frequency statics of the single-layer model and the internal pilot residual statics. Conventional residual statics improved the stack response with no data breaks.*

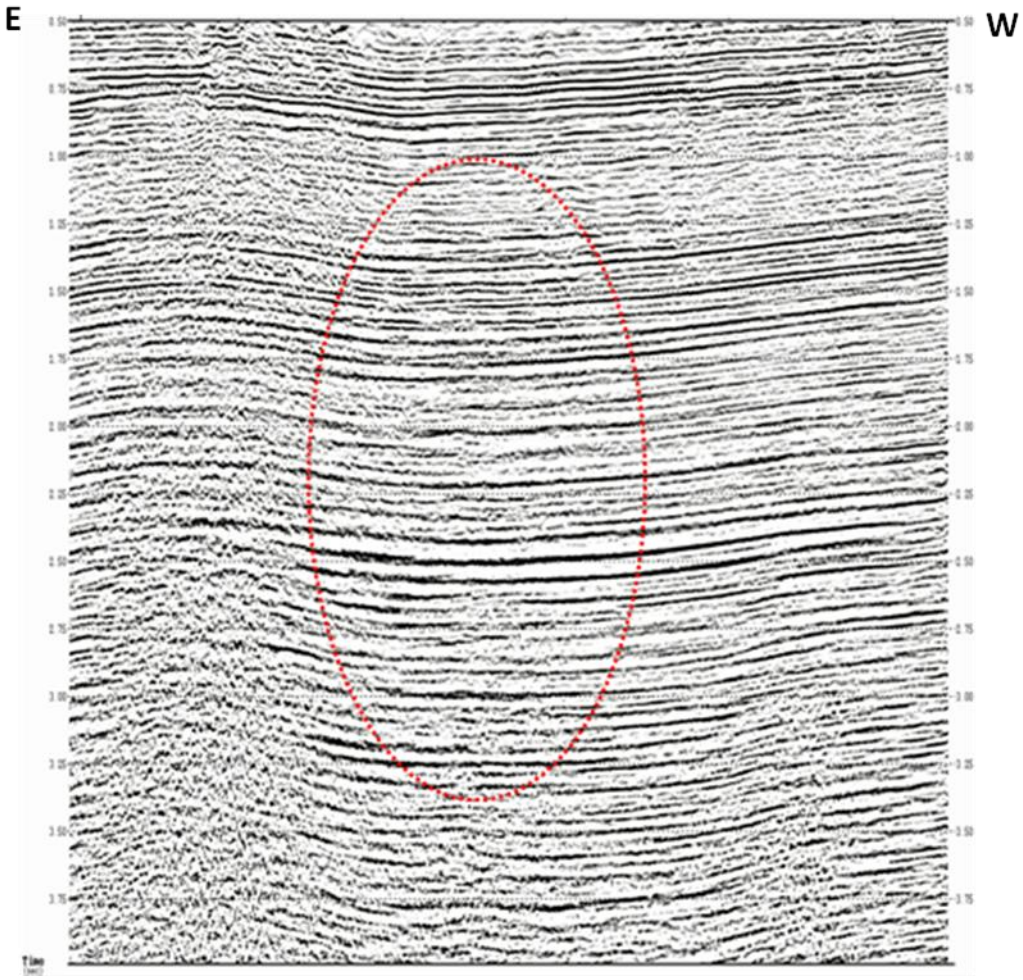


*Figure 3.6: In-line (B) stack with the high frequency statics of the multi-layer model and the internal pilot residual statics. Conventional residual statics introduced data discontinuity.*

## 3.3 Proposed Methodology

The proposed methodology is represented by the flow chart shown in Figure 3.7. The workflow is divided into two stages: the first stage is to build a data-driven external trace volume pilot using a hybrid static model (high frequency from the single-layer and low frequency from the multi-layer); the second stage is to use that pilot for residual statics. To build the external pilot, the single-layer high frequency static component is applied to the pre-stack processed data (as described in Chapter 2). One pass of the residual statics is then computed and applied to the data. The data is now ready to be stacked. The data stack response and continuity is good enough (Figures 3.3 and 3.5) to be used as a guide pilot for residual statics computations. Next, the low frequency statics from the multi-layer static model are applied to the data, which is why I called it a “hybrid static model.” To ensure that the pilot data volume was free of artificial breaks, I applied some conditioning to the stack volume, which included signal coherency using a dip coherency enhancement technique to improve the signal-to-noise ratio. I then applied a band pass filter to keep frequencies within the band of 12-62 Hz. Finally, I used time variant automatic trace scaling to balance the data. Figure 3.8 shows an in-line from the resulting data volume after applying statics (top) and the same in-line after applying the low frequency multi-layer model and the post stack data conditioning (bottom). Using that external pilot and the

input pre-stack gather data with the multi-layer model high and low frequency statics, I performed the residual statics computation. I applied those residual statics on top of the multi-layer high frequency statics to produce the skip-free data volume.

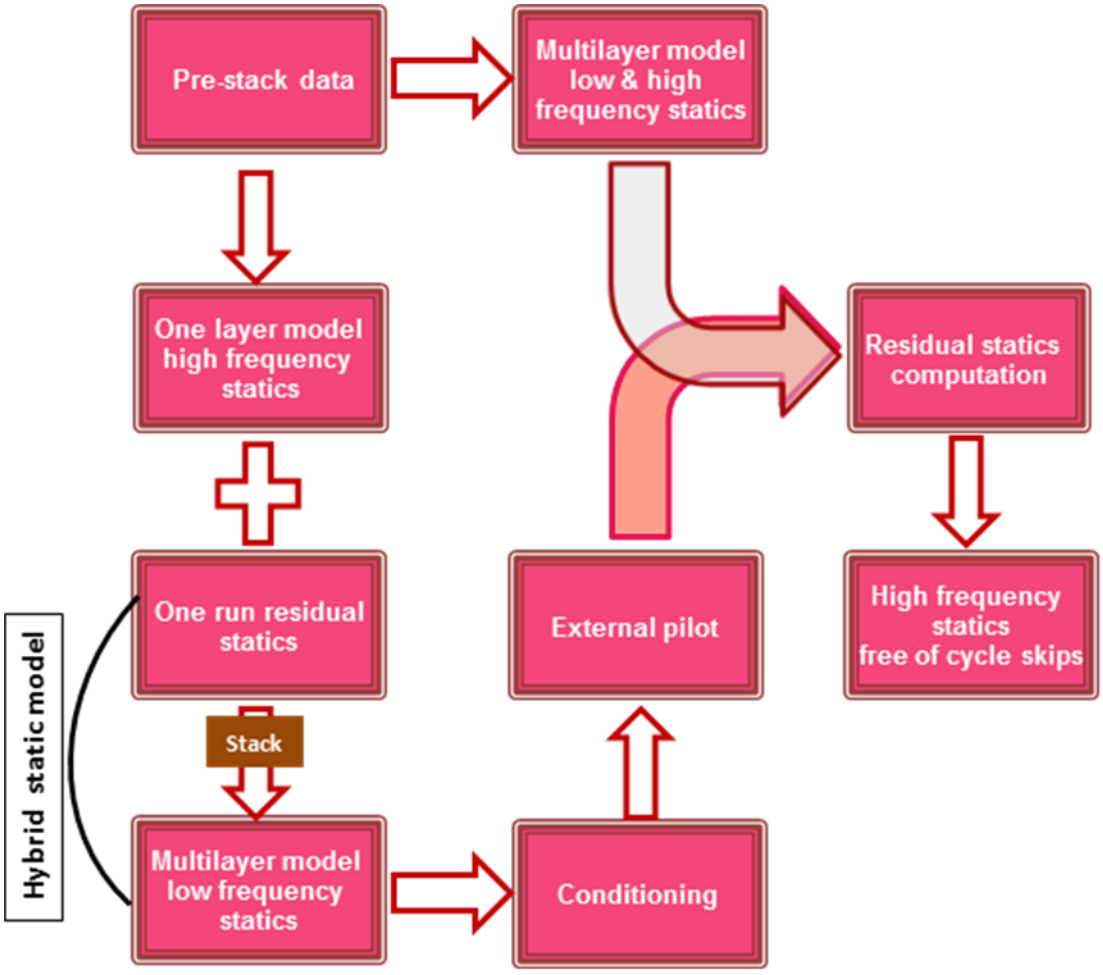


*Figure 3.7: A schematic flowchart of the proposed approach to fix statics cycle skips.*

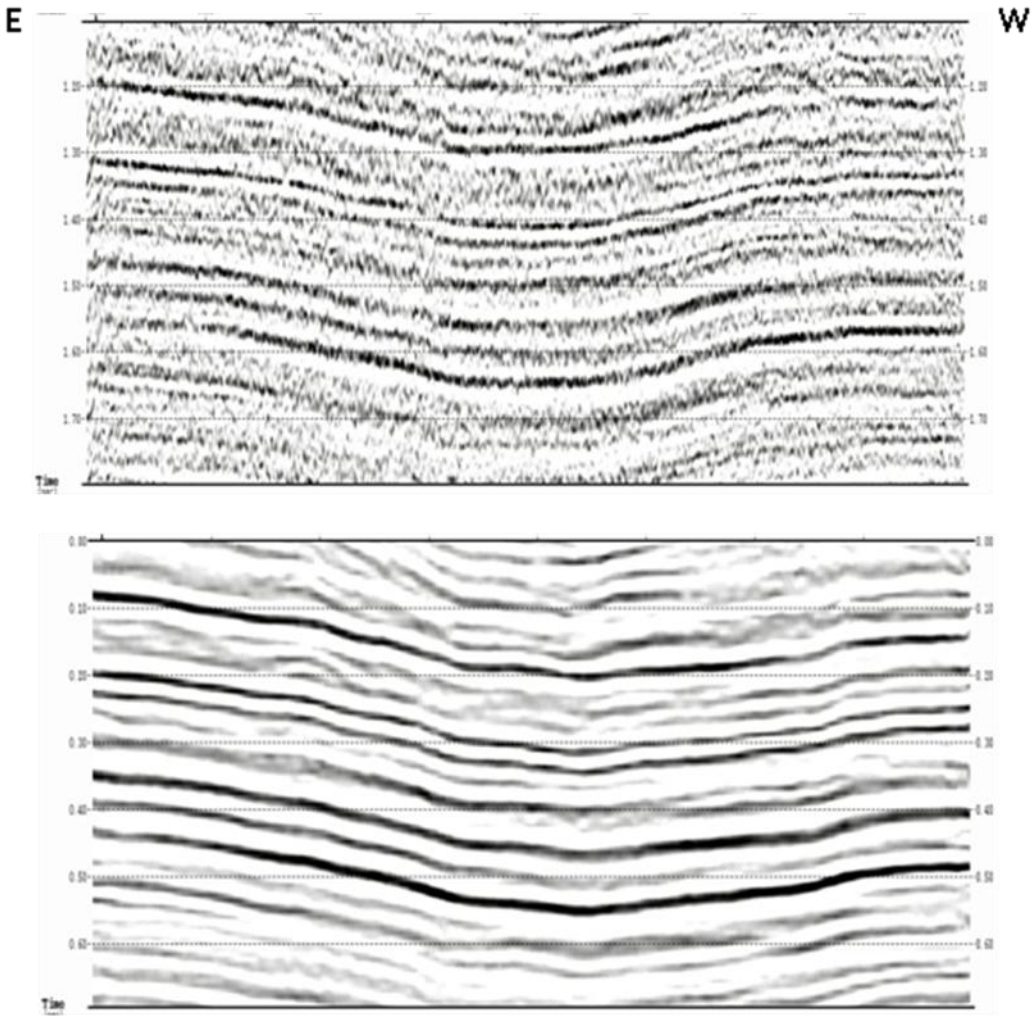


*Figure 3.8: Post-stack data conditioning: the top section is an in-line after applying the new approach statics (single-layer model high frequency statics and residual). The bottom section is the same in-line after applying low frequency multi-layer model statics and post-stack data conditioning. Data similar to the bottom line is used as an external pilot for the residual statics computations.*

# CHAPTER 4

# RESULTS

## 4.1 Introduction

The main results of these tests are summarized in this chapter in order to evaluate the method proposed to calculate residual statics that can be used for producing skip-free data volume. The results include comparisons of the applications of the new approach and the conventional approach. The comparisons include the pre-stack and post-stack data.

## 4.2 Pre-stack Data

Figure 4.1 shows an example source gather after application of the new approach (the high frequency component of the two-layer model and residual statics computed from the external pilot of the hybrid static model). It is clear that the cycle skip introduced by the conventional static solution (Figure 3.2) is resolved using the new approach.

## 4.3 Post-stack Data

Figure 4.2 shows a post-stack cross-line result where the top section is a part of the cross-line (A) using the new approach statics solution. The bottom section shows the same part using the conventional solution statics approach (multi-layer high frequency statics and internal pilot residual statics). Figures

4.3 and 4.4 show time slices along the XY plane of the 3D post-stack data volume at times 700 ms and 1400 ms, respectively. The top time slice shows the data volume after applying the new approach, whereas the bottom time slice shows the data volume after applying the conventional approach. Figures 4.5 and 4.6 show full-length cross-line (A) and in-line (B) seismic sections using the new approach.

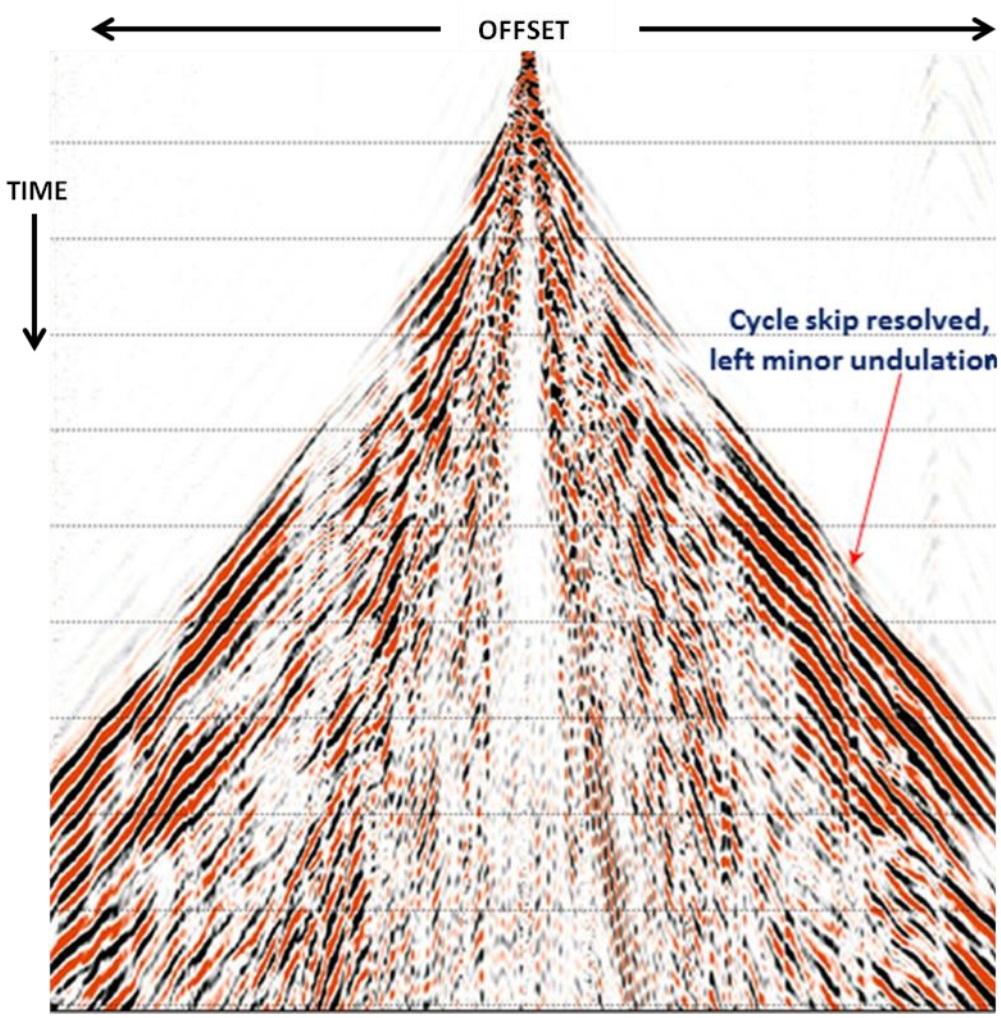


*Figure 4.1: The example source gather after applying proposed statics solution (i.e., two layer high frequency statics applied and external pilot residual statics). Note that statics cycle skip was resolved.*

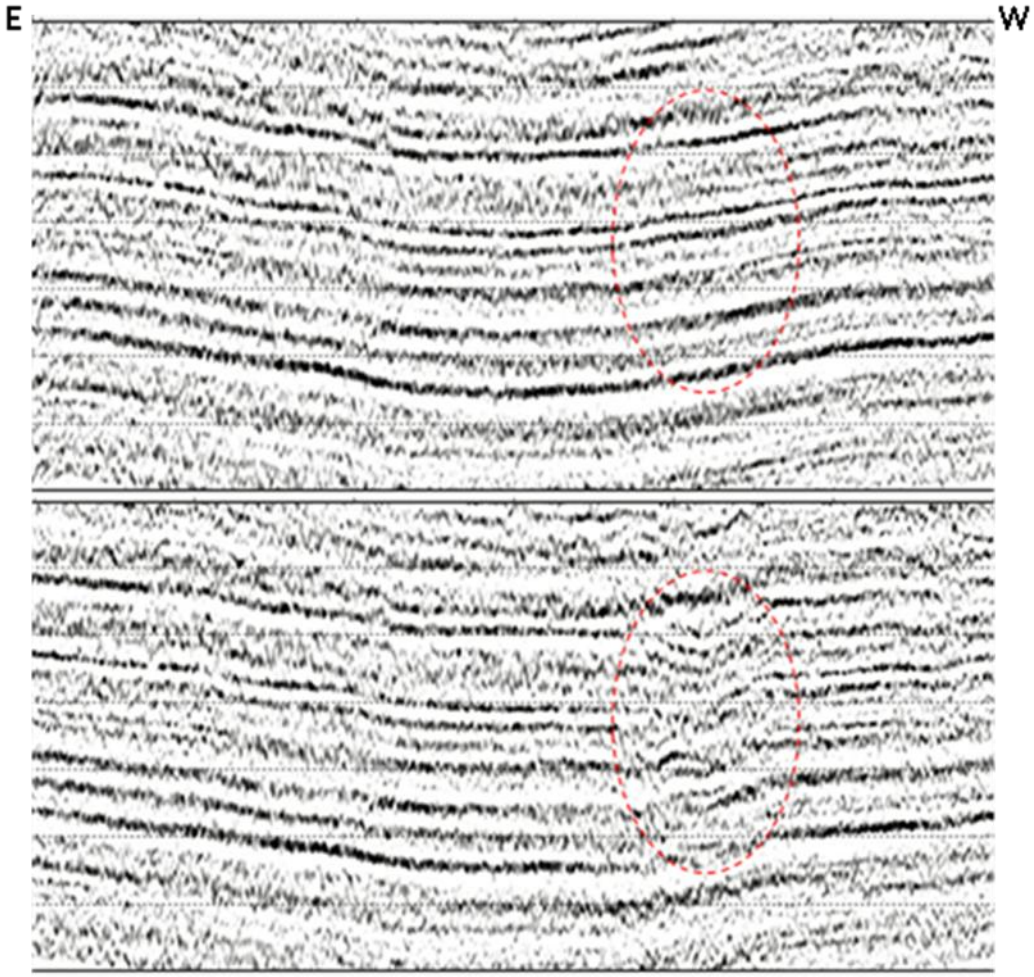


*Figure 4.2: Part of cross-line (A) stack with the new approach (top), and the conventional approach (bottom)*

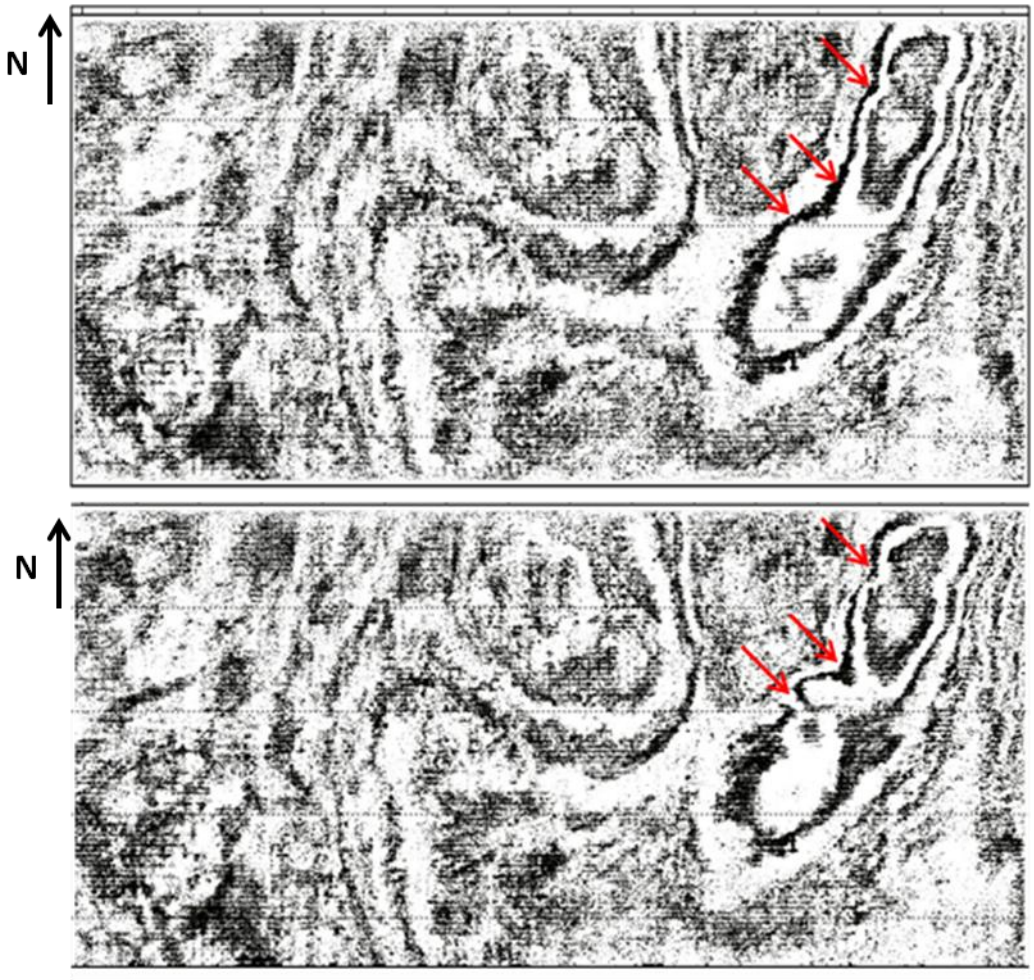


*Figure 4.3: Post-stack volume time slice at 700 ms in the XY direction: the proposed statics solution (top) and the conventional statics solution (bottom). The arrows indicate places where the data showed cycle skips.*

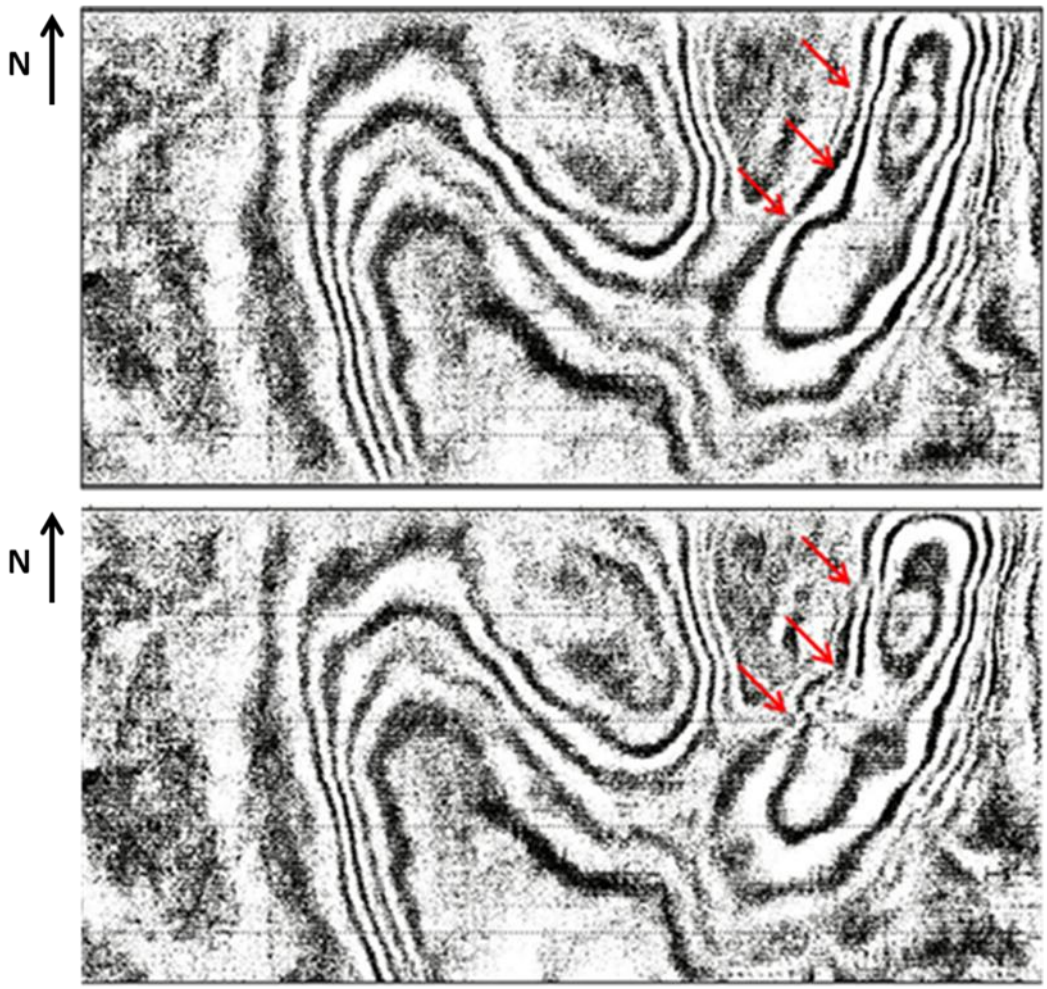


*Figure 4.4: Post-stack volume time slice at 1400 ms in the XY direction. Proposed statics solution (top) and conventional statics solution (bottom). Arrows indicate places where data showed cycle skips.*

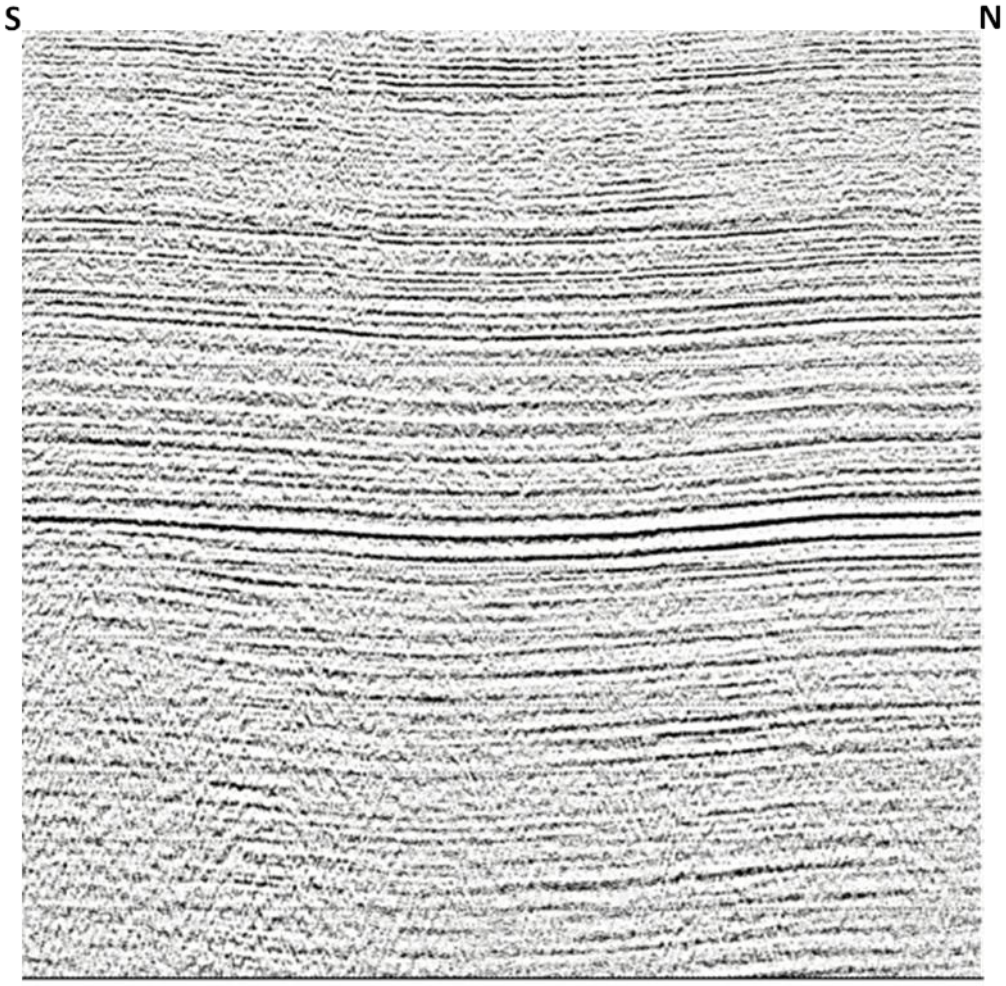


*Figure 4.5: Full seismic section in the cross-line direction (cross-line A). Proposed statics solution resulted in reasonable data continuity with no cycle skips.*

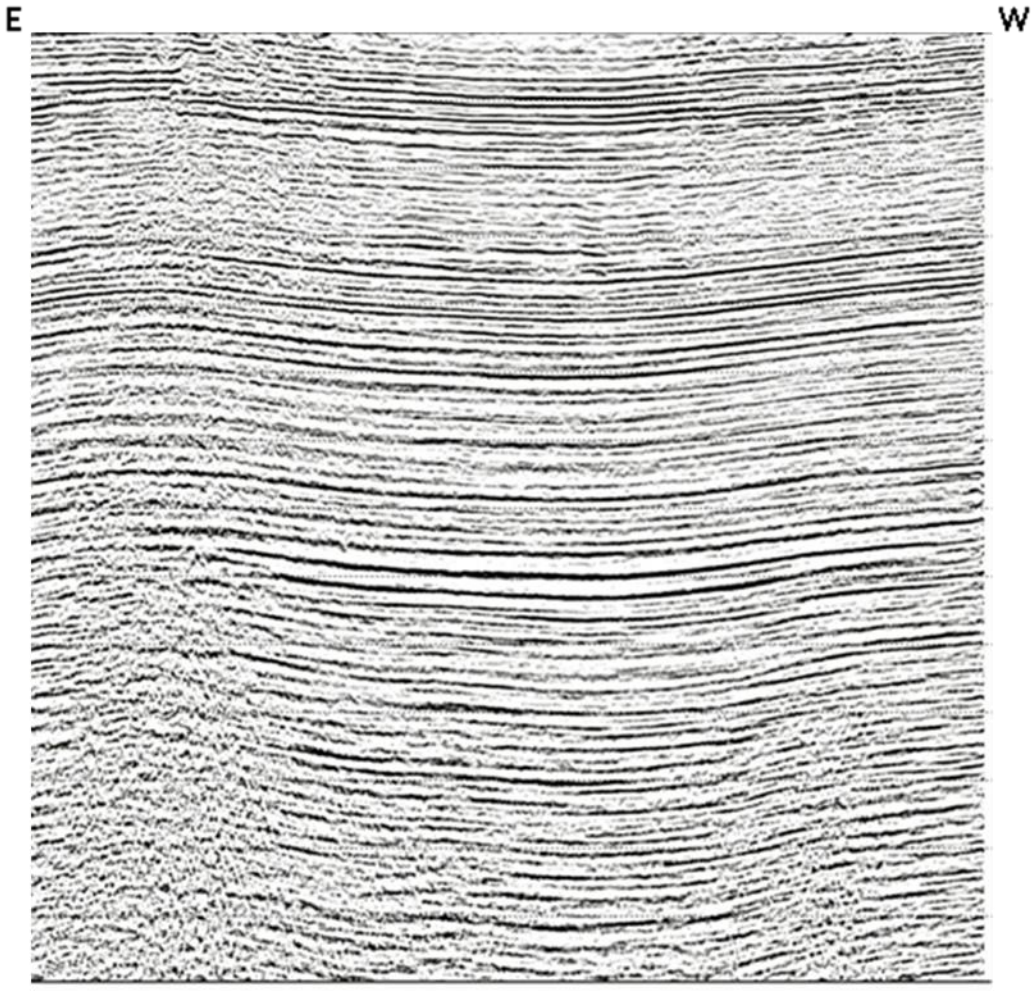


*Figure 4.6: Full seismic section in the in-line direction (in-line B). Proposed statics solution resulted in reasonable data continuity with no cycle skips.*

# CHAPTER 5

# CONCLUSIONS AND RECOMMENDATIONS

## 5.1 Conclusions

The multi-layer static model resolves many major static problems across the Kingdom of Saudi Arabia. This model is more realistic than the single-layer static model as it represents the velocity of the weathering and few sub-weathering layers compared with the single-layer, which averages all these velocities. In some areas, the one-layer static model shows better continuity than the multi-layer static model because the latter model introduced cycle skips and artificial data breaks. The reason for these cycle skips might be that the multi-layer model uses horizontal ray paths whereas the single-layer model uses vertical ray paths, which is particularly important in the case of the velocity inversion and shallow buried anomaly.

After the application of statics, quality control is very important and is achieved by examining the data in various directions. In our case study, major cycle skips in data volume were obvious and more easily detectable in the cross-line direction on both the cross sections and the time slices than on the in-line direction. Examination of the in-line seismic sections was misleading as it showed no data break or cycle skip.

My approach provides a tool that hybridizes the single-layer static model (high-frequency static component) with the multi-layer static model (low-

frequency static component). This static combination is used to form a smooth model that can be used as an external pilot to correct the cycle skips in the data. A critical point that made this approach successful is the addition of a skip-free external pilot to the residual static program to calculate statics, which when applied to the input traces, produced highly continuous data with no artificial data breaks.

Represented by the time slices of cross-lines and in-lines, the final results clearly showed that the data breaks caused by the internal pilot residual statics calculation affected the integrity of the whole structural closure, particularly at the 1400 ms time slice.

## 5.2 Recommendations

Although the multi-layer static model is preferable to the single-layer static model in seismic data processing, the single-layer static model should always be used in addition to the multi-layer model static stack model to produce a seismic volume. This kind of quality control should always be done to compare the results of the application of the two static models. In-line, cross-line and time slices should be produced and examined thoroughly for both the single-layer and the multi-layer model stack volumes to check the data for any artificial discontinuity or any possible cycle skips.

Before using the proposed hybrid approach to resolve cycle skips introduced by the multi-layer model, one should try to resolve the static problem by

running the regular internal pilot residual statics techniques. Many trials should be done using different combinations of residual statics parameters to determine whether those residual statics trials resolve or worsen the static problem.

# Bibliography


Bridle, R. (2009) Delay time refraction methods applied to a 3D seismic block. *The Leading Edge*, **28**, 260-269.

Bridle, R., Ley II, R., Al-Mustafa, A., and Pittman, M. (2005) Evolution of a near-surface model in an area of complex topography. Expanded Abstracts, 75th Annual International Meeting, SEG, pp. 2225-2228.

Buck, A.V., Al-Dulaijan, A.Y., Al Yacoub, T., and Al Ghamdi, S. (1996) Near surface modeling in Saudi Arabia. Extended Abstracts, 58th Annual Meeting, EAGE, B037.

Butler, D.K. (2005) What is near-surface geophysics. In D.K. Butler, ed. *Near-Surface Geophysics*, SEG, pp. 1-6.

Cox, M. J. G. (1999) *Static Correction for Seismic Reflection Surveys*. SEG, Tulsa.

Cunningham, A.B. (1974) Refraction data from single-ended refraction profiles. *Geophysics*, **39**, 292-301.

Danbom, S.H. (2005) Special challenges associated with the near-surface. In Butler, D.K., ed., *Near-Surface Geophysics*. SEG, pp. 7-30.

Hatherly, P.J., Urosevic, M., Lambourne, A., and Evans, J.B. (1994) A simple approach to calculating refraction statics corrections. *Geophysics*, **59**, 156-160.

Knox, W.A. (1967) Multi-layer near-surface refraction computations. In A.W. Musgrave, ed. *Seismic Refraction Prospecting*, SEG, pp. 197-216.

Ley II, R., Bridle, R., Amarasinghe, D., Al-Homaili, M., Al-Ali, M., Zinger, M., and Rowe W. (2003) Development of near-surface models in Saudi Arabia for low relief structures and complex near-surface geology. Expanded Abstracts, 1992-1995. 73rd Annual International Meeting, SEG, pp. xx.

Palmer, D. (1986) *Refraction Seismics: Handbook of Geophysical Exploration*. Vol 13. Geophysical Press .

Sheriff, R. E. (1977) Limitations on resolution of seismic reflections and geologic detail derivable from them. In C.E. Payton, ed. *Seismic Stratigraphy: Applications to Hydrocarbon Exploration*. AAPG, pp. xx.

Yilmaz, O., (1987) *Seismic Data Processing*. SEG.

Zhang, J. and Yilmaz, O. (2005) Near-surface corrections for complex structure imaging. Expanded Abstracts, 75th Annual International Meeting, SEG, pp. 2566-2568.

# Vita

Emad Ekladios Toma Tawadros hold Egyptian and Australian nationalities, was born in Cairo, Egypt on July 29, 1966. In 1988, he received a double major Bachelor of Science degree with honors in geology and chemistry from Ain Shams University. He then worked for the Land and Water Institute as a researcher for a year. In 1992, he joined the Western Geophysical Data Processing Centre in Cairo, Egypt, as a processing geophysicist where he processed land and marine seismic projects. He immigrated to Australia in 1997, and joined the Western Geophysical Data Processing Centre in Perth, where he processed 2D and 3D marine and land seismic data. In 2001, he joined Saudi Aramco as a seismic data processor; currently he is a seismic data geophysical specialist where he processes varieties of seismic data. Mr. Tawadros is a member of SEG and EAGE.

His permanent address is 2603/90 Lorimer Street Docklands, VIC 3008, Melbourne, Australia. Mr. Tawadros currently lives at 514 Safwa Lane, Dhahran hills camp, Saudi ARAMCO, Dhahran.. P.O. BOX 12804 Dhahran, 31311. His phone contacts are; cell+966-507823992, office +966-3873-4096.

His email addresses are; emad.tawadros@aramco.com, tawadrose@yahoo.com.